Article published online: 2024-08-05

Imaging in Musculoskeletal TB

Stanzin Spalkit[1] Ankur Goyal[1] Shivanand Gamanagatti[1] Devasenathipathy Kandasamy[1] Raju Sharma[1]

[1] Department of Radiodiagnosis and Interventional Radiology, All India Institute of Medical Sciences, New Delhi, India

Indographics 2024;3:100–120.

Address for correspondence Ankur Goyal, MD, DNB, MNAMS, FICR, FESUR, Department of Radiodiagnosis and Interventional Radiology, All India Institute of Medical Sciences, Sri Aurobindo Marg, Ansari Nagar, Ansari Nagar East, New Delhi 110029, India (e-mail: ankurgoyalaiims@gmail.com).

Abstract

Tuberculosis (TB) remains a significant global health challenge, with musculoskeletal TB accounting for a notable proportion of cases. The spine is the most commonly affected site, followed by the hip, knee, and ankle joints. Prompt and accurate diagnosis is essential to prevent joint destruction, deformity, and neurological complications. Given the paucibacillary nature of musculoskeletal TB, imaging plays a pivotal role in diagnosis, guiding sampling procedures, and assessing treatment response. Contrast-enhanced magnetic resonance imaging has emerged as the preferred modality for diagnosing and monitoring both spinal and extraspinal TB. This review provides an in-depth analysis of imaging characteristics of musculoskeletal TB, highlighting key findings essential for early diagnosis and differentiation from similar pathologies. Through case-based illustrations, various anatomical locations of osteoarticular TB are discussed.

Keywords

- TB
- musculoskeletal
- MRI
- bone TB
- joint TB
- osteoarticular

Introduction

Tuberculosis (TB) remains a major public health problem worldwide and a significant cause of morbidity and mortality.[1] According to the World Health Organization, an estimated 10.6 million people fell ill with TB in 2021, and 1.6 million people died from the disease.[2] The emergence of multidrug-resistant TB and the high prevalence of human immunodeficiency virus (HIV) coinfection have further complicated the global TB epidemic.[3]

Musculoskeletal TB accounts for approximately 1 to 3% of all TB cases and up to 10 to 15% of extrapulmonary TB cases.[4] The spine is the most common site of musculoskeletal TB, accounting for approximately 50% of cases, followed by the hip, knee, and ankle joints. Other less common sites include the shoulder, elbow, wrist, and small bones of the hands and feet.[5] Musculoskeletal TB can also involve the soft tissues, such as the tenosynovium, bursae, and muscles.[6]

The incidence of musculoskeletal TB has been increasing in recent years, particularly in developing countries and among immunocompromised individuals. Delayed management of musculoskeletal TB can lead to joint destruction, deformity, and neurological complications.[7] Therefore, early and accurate diagnosis is crucial for the successful management of these cases.

Pathogenesis and Predisposing Factors

Causative Microorganisms

Musculoskeletal TB is primarily caused by *Mycobacterium tuberculosis*, with a small percentage of cases attributed to *Mycobacterium bovis*.[8] Atypical mycobacteria (such as *Mycobacterium kansasii*, *Mycobacterium marinum*, *Mycobacterium scrofulaceum*, and *Mycobacterium avium* complex) account for approximately 1 to 4% of TB cases.[9]

DOI https://doi.org/10.1055/s-0044-1787773.
ISSN 2583-8229.

Thieme Medical and Scientific Publishers Pvt. Ltd., A-12, 2nd Floor, Sector 2, Noida-201301 UP, India

Microbiology and Histopathology

The diagnosis of musculoskeletal TB relies on identifying the causative organism through microbiological and histopathological examinations. Mycobacterial culture remains the gold standard for diagnosis, allowing for species identification and drug susceptibility testing. The traditional method of TB culture on the Lowenstein–Jensen (LJ) medium has been superseded by automated liquid culture systems, with Mycobacterial Growth Indicator Tube (MGIT) being the favored option. MGIT offers faster results and improved detection rates. Moreover, it can also be utilized for both culture and drug sensitivity testing. However, due to the notable contamination rates associated with MGIT cultures, LJ culture is concurrently conducted as a safeguard.[10]

Nucleic acid amplification tests (NAATs), such as the Xpert MTB/RIF assay, rapidly detect *M. tuberculosis* and rifampicin resistance.[11]

Histopathological examination of biopsy specimens is crucial for diagnosing extrapulmonary TB, as these forms are often paucibacillary with negative acid-fast bacillus (AFB) stains and cultures. The hallmark of TB infection is necrotizing granulomatous inflammation.[12]

Joint fluid aspirate reveals elevated proteins ($>$ 2.5 g/100 mL), decreased sugar level (less than 50 mg/100 mL), and increased white cell count (in the inflammatory range, typically 10–20 $\times$ 10^9/L) with lymphocytosis.[13] AFB stains are usually negative. Synovial fluid culture is positive in only approximately 20 to 40% of cases. NAATs for TB reveal high sensitivity and specificity.[14] They offer a quick and dependable diagnosis for TB, notably surpassing the time taken by traditional culture methods. Its effectiveness is particularly pronounced with samples containing low levels of bacteria, like smear-negative osteoarticular specimens.[15,16]

Spread of Infection

Musculoskeletal TB most commonly results from hematogenous dissemination or lymphatic spread from a primary or reactivated infected focus, usually in the lungs or genitourinary system. Direct inoculation or contiguous spread from adjacent infected tissues occurs less frequently. The rich vascular supply of the vertebrae and the growth plates of long bones in children make these sites particularly susceptible to hematogenous spread.[6]

Predisposing Factors

Several factors can predispose individuals to musculoskeletal TB, including immunosuppression (particularly HIV infection), poor socioeconomic conditions, malnutrition, and comorbidities such as diabetes mellitus and chronic kidney disease. Previous joint disease, trauma, or surgery may also increase the risk of developing musculoskeletal TB.[1]

Manifestations of Musculoskeletal TB

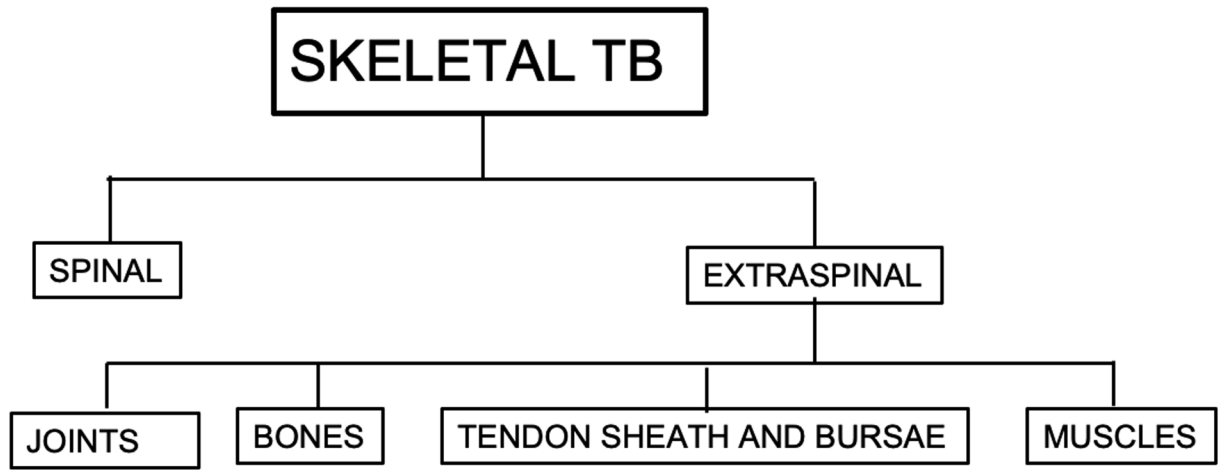

Spinal Tuberculosis

Pathogenesis

Spinal TB, also known as Pott's disease, is the most common form of musculoskeletal TB, accounting for approximately 50% of cases.[17] The infection typically starts in the anterior aspect of the vertebral body, near the endplate, due to the rich vascular supply in this region. The most common route of infection is hematogenous spread from a primary focus. Less commonly, direct extension from adjacent infected tissues, such as the pleura or psoas muscle, can occur.[18]

The infection initially causes granulomatous inflammation and caseous necrosis in the vertebral body, leading to trabecular and cortical bone destruction. The infection can spread to the adjacent intervertebral disc (IVD) as the disease progresses, causing disc destruction and collapse. The infection may also extend into the paraspinal soft tissues, forming cold abscesses. In advanced cases, the structural integrity of the spine can be compromised, leading to kyphotic deformity and spinal instability.[19] The thoracolumbar region is the most commonly affected site, while the cervical and sacrum regions are less commonly involved.[9]

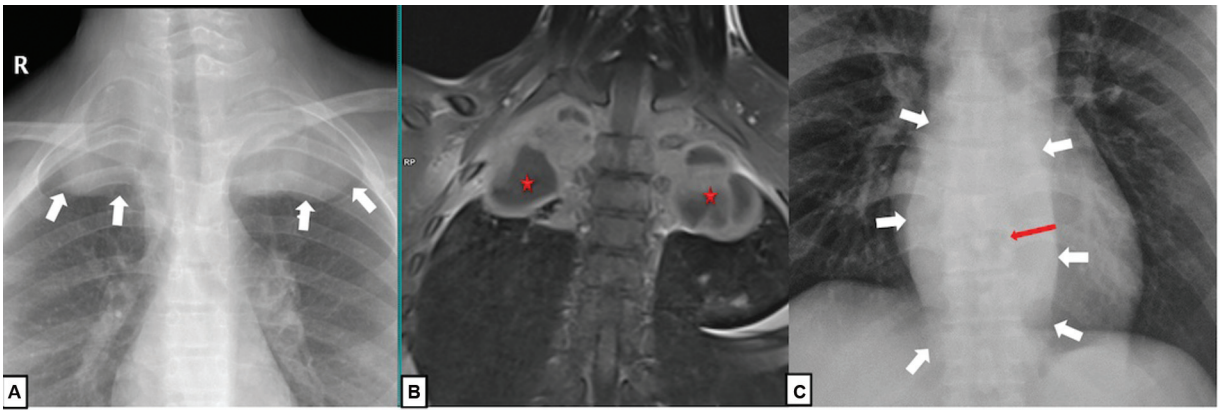

Fig. 1 Paravertebral opacities. Chest radiograph (**A**) shows a widening of the superior mediastinum and opacities extending to both lung apices (arrows). Coronal postcontrast T1-weighted (T1W) magnetic resonance imaging (MRI) image (**B**) shows large bilateral paravertebral peripherally enhancing collections (star) adjacent to the upper dorsal spine. Chest radiograph of another patient (**C**) showing fusiform retrocardiac opacity (white arrows), close observation reveals D11 vertebral body collapse and D10-11 intervertebral (IV) disc space loss (red arrows)—bird's nest appearance of the paravertebral collection.

Clinical Presentation

The clinical presentation is often insidious, with the most common symptoms being back pain, fever, weight loss, and neurological deficits. Constitutional symptoms, such as fever, night sweats, and weight loss, are present in 20 to 30% of patients.[20]

Neurological deficits can occur due to spinal cord compression from epidural extension of the infection, kyphotic deformity, or spinal instability. Patients may also present with signs and symptoms related to the primary site of infection, such as pulmonary or genitourinary symptoms.[21]

Imaging Features

Radiography

Radiography is insensitive to early detection of tuberculous spondylodiscitis, as up to 50% of bone destruction may occur before changes are visible on radiographs.[22]

Early findings include localized osteopenia and loss of the vertebral endplate cortical definition. Relative sparing of the IVD height is a characteristic feature of early stage of tuberculous spondylodiscitis due to the lack of proteolytic enzymes responsible for its early damage in cases of pyogenic spondylitis.[7]

Pre-/paravertebral collection or granulation tissue is seen on the radiograph as a soft tissue mass, which may manifest as follows[23,24]:

- Cervical spine: increased prevertebral soft tissue thickening on the lateral view, measuring greater than 5 mm above and 15 mm below the cricoid cartilage level.[25]
- Upper dorsal spine: widening of the superior mediastinum on anteroposterior view and altered tracheal contour on lateral view (►**Fig. 1**).
- Lower dorsal spine (below D4 level): posterior mediastinal mass (may have fusiform bird's nest-type appearance) (►**Fig. 1**).
- Lumbar spine: poorly demarcated psoas margin.

Anterior subligamentous spread of disease on radiograph is seen as anterior vertebral scalloping of multiple contiguous vertebrae on the lateral radiograph. As the disease progresses, radiographs may demonstrate vertebral body destruction, collapse, and kyphotic deformity[21] (►**Fig. 2**). Paravertebral soft tissue masses and calcifications may be visible in advanced cases. Calcification within a collection is highly suggestive of TB.[24]

Tubercular involvement of posterior elements can be suggested by indirect signs such as nonvisualization of pedicle or spinous process, spondylolisthesis due to involvement of facet joints or pars interarticularis, and paraspinal soft tissue mass in the absence of vertebral erosions.[26]

The utility of radiographs is limited in areas of complex anatomy such as craniovertebral and cervicodorsal junction.[27]

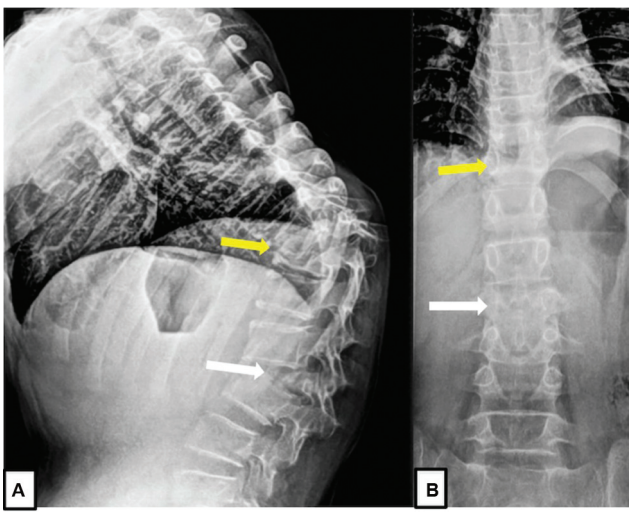

Fig. 2 Tuberculosis (TB) spine radiographs—kyphotic deformity. Radiograph dorsal spine lateral (**A**) and anteroposterior (AP) view (**B**) showing focal kyphotic deformity at the lower dorsal level due to collapse of multiple contiguous vertebrae (D10–D12) with loss of intervening intervertebral (IV) discs (yellow arrow). Complete collapse of L3 vertebral body also seen (white arrow), suggesting multifocal disease.

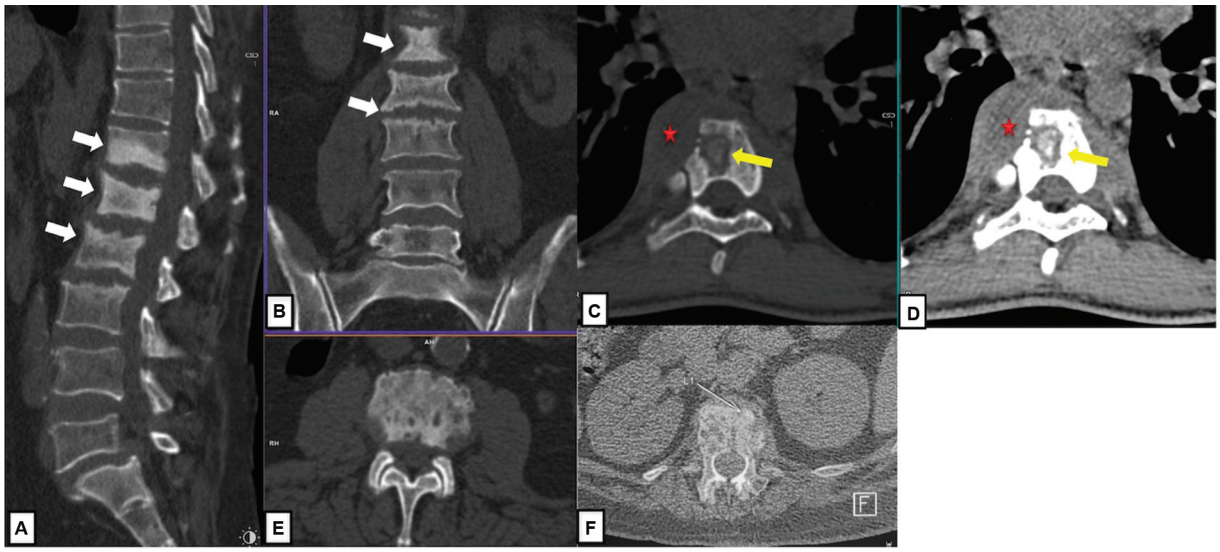

Fig. 3 Patterns of tuberculosis (TB) spine on computed tomography (CT). Sagittal and coronal CT bone window dorsolumbar spine (**A** and **B**, respectively) show sclerosis of D12 to L3 vertebrae with endplate erosions and reduced vertebral height—sclerotic pattern. Axial bone and soft tissue window at middorsal spine level (**C** and **D**) show central osteolytic lesion (arrow) with hyperdense dead bone (sequestrum) within. There is associated pre- and paravertebral collection (star) which is more conspicuous on the soft tissue window, causing scalloping of the anterior surface of the vertebral body. Axial bone window and soft tissue window images (**E** and **F**, respectively) of the lumbar vertebrae in two different patients show fragmentary patterns of destruction which is the most common pattern.

Computed tomography

Computed tomography (CT) is more sensitive than radiographs in detecting early bone destruction, paravertebral collections, and spinal canal involvement. Four patterns of bone destruction have been described on CT; fragmentary, osteolytic, sclerotic, and subperiosteal[28] (►**Fig. 3**). It plays a vital role in revealing calcification within a collection or bone fragments within epidural collection.[29] However, a notable drawback is its inability to detect marrow changes indicative of disease activity especially when overt collections are absent and spinal cord compression. It is particularly valuable for guiding percutaneous diagnostic sampling, especially in challenging-to-access areas[30] (►**Fig. 4**).

Magnetic Resonance Imaging

Magnetic resonance imaging (MRI) is the imaging modality of choice for a comprehensive assessment of tuberculous spine, especially for examining challenging areas such as the craniovertebral junction, cervicodorsal junction, neural arch elements, vertebral appendages, sacroiliac joint region, sacrum, and coccyx.[30] It provides unique insight into disease activity, making it indispensable for evaluating treatment response following antitubercular therapy (ATT).[31]

Typical MRI protocol for evaluation of suspected infection of the spine includes T1-weighted (T1W) and fat-suppressed T2-weighted (T2W) sequences in sagittal and axial planes, along with short tau inversion recovery (STIR) sequences in

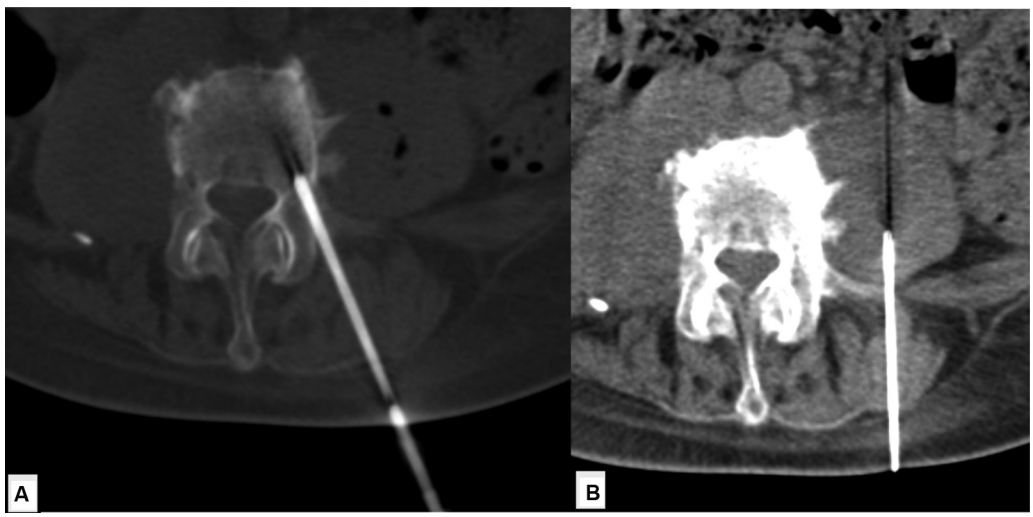

Fig. 4 Image guidance for procedures. Axial computed tomography (CT) sections through pathological vertebrae show (**A**) 11-G bone biopsy needle inserted via the left transpedicular approach in lumbar spine and (**B**) CT in soft tissue window showing bilateral paravertebral collections, thick bore (18-G) lumbar puncture (LP) needle is used to drain the collection for both diagnostic and therapeutic purpose.

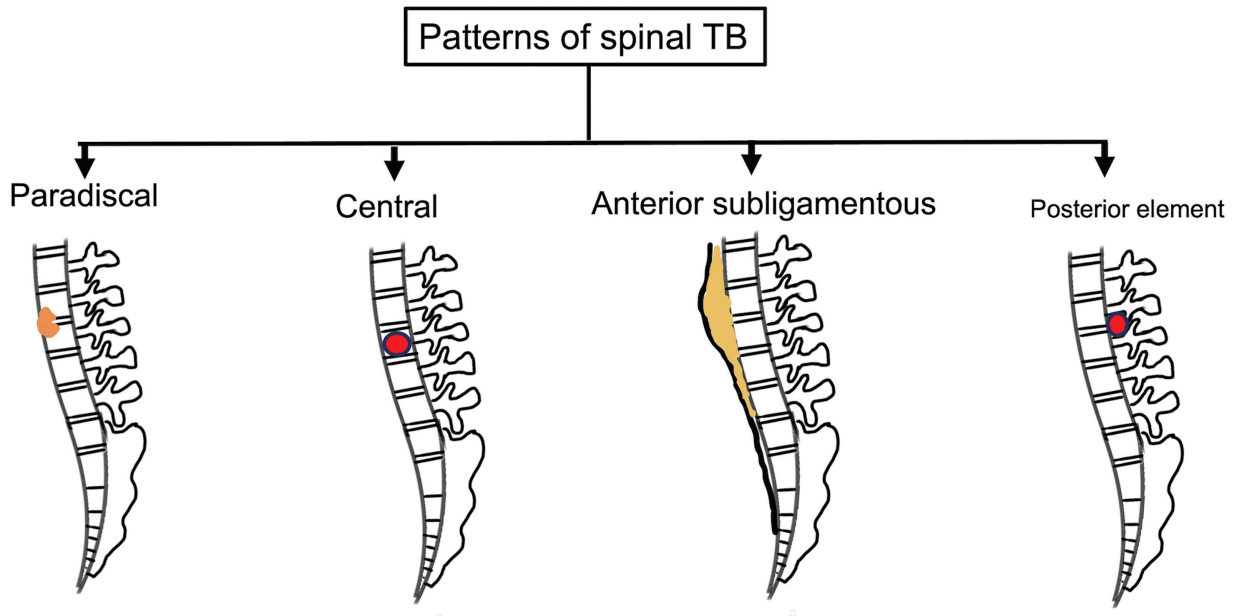

Fig. 5 Schematic representation of patterns of involvement in spinal tuberculosis.

coronal planes. Axial T2W (without fat suppression) images may be required for evaluation of spinal cord and arachnoiditis. Additionally, contrast-enhanced T1-weighted fat-suppressed sequences are acquired in at least two planes (sagittal and axial) post-gadolinium contrast injection.[32] The whole spine should be included in the sagittal acquisition to detect unsuspected multifocal disease and axial scans may be done for the abnormal area.

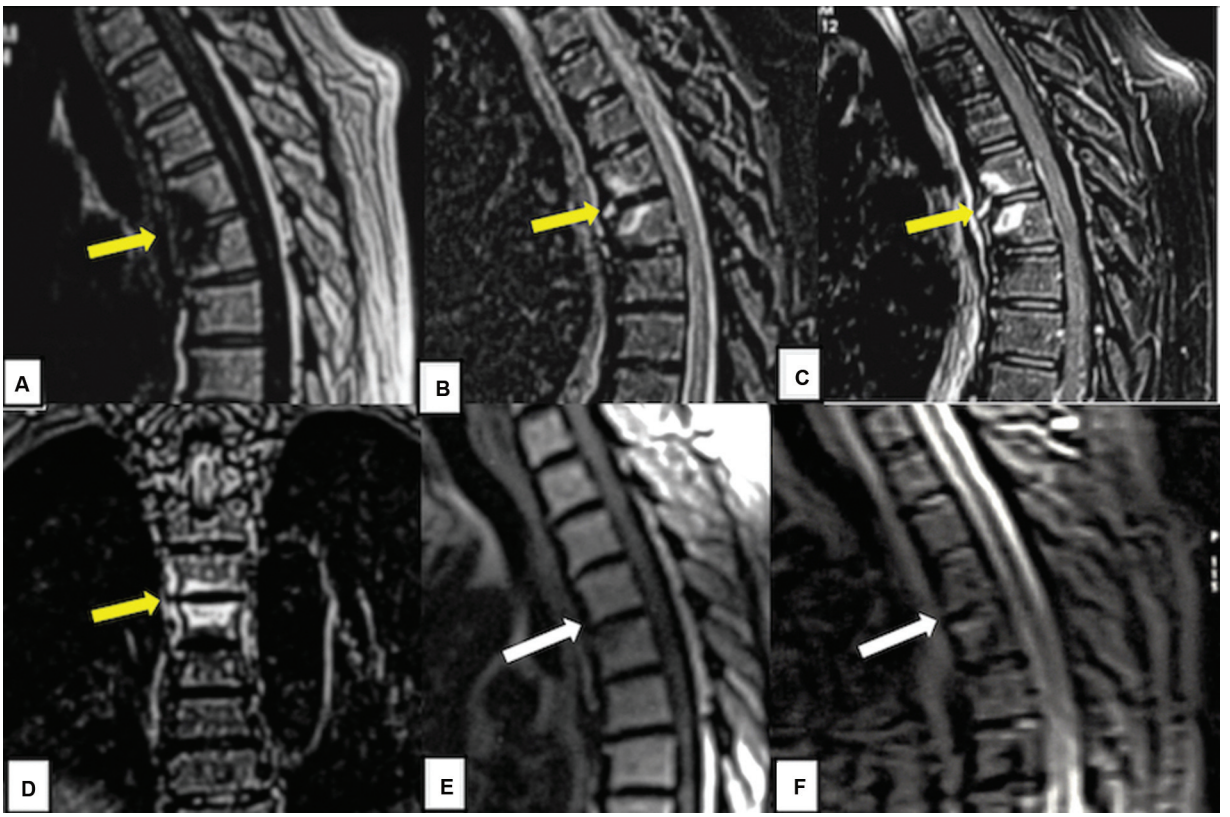

Fig. 6 Paradiscal pattern—early-stage tuberculosis (TB) spine: Sagittal T1 (**A**) and T2 (**B**) dorsal spine images show T1 hypointense, T2 fat-suppressed (FS) hyperintense signal alteration limited to the anterior sub-endplate location of two contiguous vertebrae with relative sparing of the intervening intervertebral (IV) disc (yellow arrows). Postcontrast T1 FS sagittal (**C**) and coronal (**D**) images show abnormal postcontrast enhancement in the same site. No prevertebral/epidural collection or vertebral height collapse was seen. Posttreatment imaging: Sagittal T1 non-FS and T2 FS (**E** and **F**) images show near complete resolution of the signal changes seen as fatty replacement of the affected vertebrae with only thin sub-endplate T2 hyperintensity which may persist, however, does not signify active disease (white arrow).

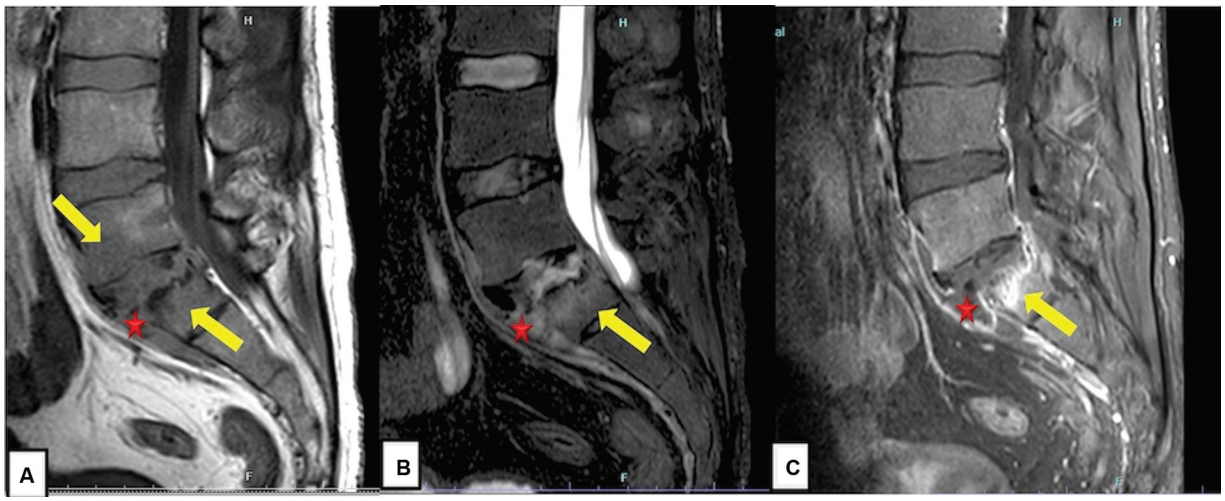

Fig. 7 Paradiscal disease pattern. Sagittal T1 non-fat-suppressed (FS) (**A**) and T2 FS (**B**) lumbosacral spine images show T1 hypointense and T2 FS hyperintense signal alteration in the sub-endplate location of two contiguous vertebrae at the L5/S1 level (yellow arrows) along with involvement of the intervening intervertebral (IV) disc and destruction of the endplate cortex. Postcontrast T1 FS sagittal (**C**) image shows abnormal postcontrast enhancement in the corresponding area showing signal alteration. A small adjacent presacral collection (star) is also seen.

Findings depend on the pattern of involvement (►**Fig. 5**):

- *Paradiscal*: This is the most common pattern and occurs due to a common arterial blood supply to this region with simultaneous involvement of two contiguous vertebrae adjacent to the IVD. The involved vertebra shows altered marrow signal intensity appearing hypointense on T1W and hyperintense on T2W sequences, heterogeneous enhancement with loss of cortical definition. The changes are predominantly epicentered in the sub-endplate location. Intervening disc involvement is seen as the loss of normal intranuclear cleft, an increased signal on T2-weighted/STIR images, and postcontrast enhancement[33] (►**Figs. 6** and **7**).

Pre-/paravertebral or epidural extension is a characteristic feature of TB and manifests in the form of either granulation tissue or collection formation. Both appear hyperintense on T2W (►**Fig. 8**).[34] The former shows homogenous enhancement while the latter reveals peripheral enhancement with a nonenhancing center. Paraspinal collections tend to track along areas of low resistance, along intercostal space in case of dorsal spine involvement, and along the psoas muscle in lumbar spine involvement. Psoas involvement is seen as increased bulk

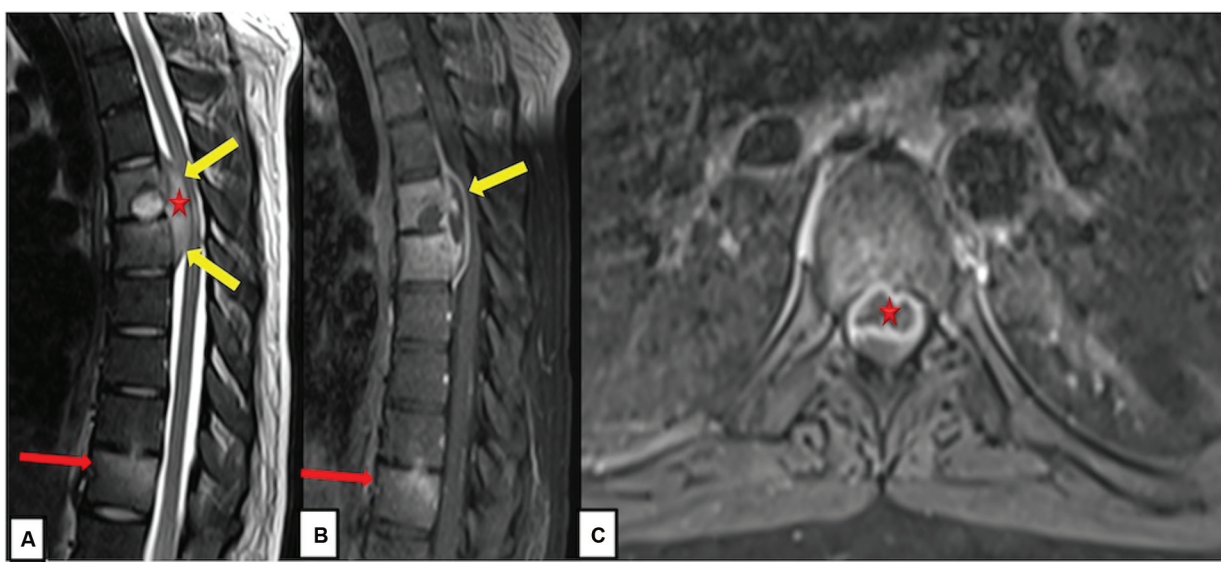

Fig. 8 Epidural collection and skip lesion on magnetic resonance imaging (MRI): Sagittal T2-weighted (T2W) (**A**), sagittal and axial postcontrast T1W (**B** and **C**) images show upper dorsal paradiscal disease, sub-endplate erosion with adjacent prominent focal epidural collection lifting the posterior longitudinal ligament causing significant canal compromise and dorsal cord compressive myelopathy. Another focal vertebral signal alteration showing abnormal postcontrast enhancement was seen in the lower dorsal spine (red arrow).

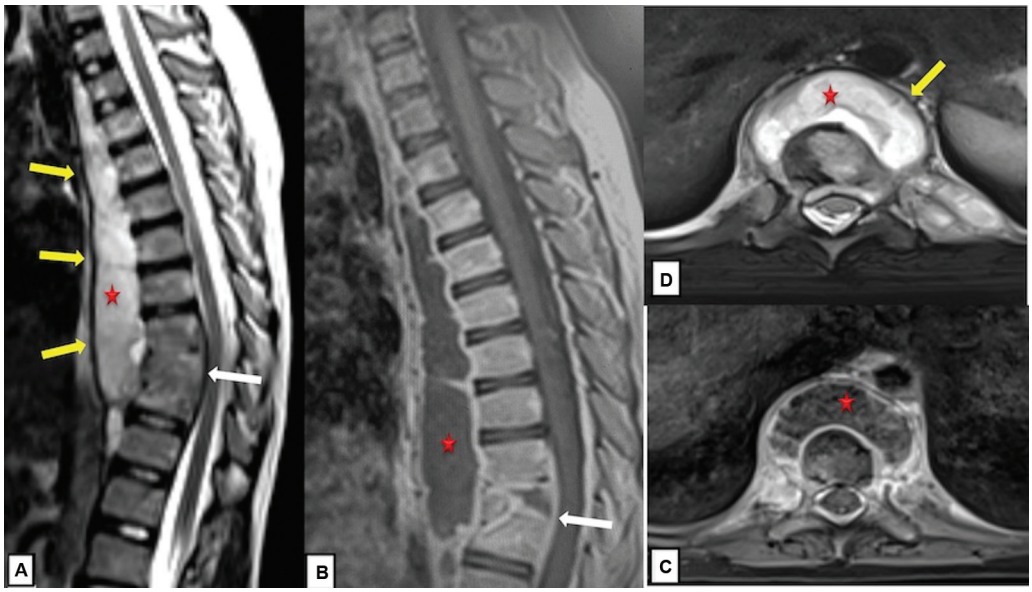

Fig. 9 Anterior subligamentous pattern. T2 and T1 postcontrast sagittal (**A** and **B**) and axial images (**C** and **D**) show a large peripherally enhancing collection (star) uplifting and anteriorly displacing the anterior longitudinal ligament (yellow arrows) and extending longitudinally. Note multiple contiguous vertebral extensions with maintained intervertebral (IV) discs except in the lower dorsal spine which shows a paradiscal pattern of involvement (white arrow).

and loss of normal muscle morphology, T2/STIR hyperintensity with peripherally enhancing collection within it or along its fascia.[35]

- *Anterior subligamentous pattern*: This occurs when the disease spreads to multiple contiguous vertebrae deep to the anterior longitudinal ligament (ALL), thus involving the anterior aspect of the vertebral body. It differs from the paradiscal pattern as discal involvement and vertebral collapse are minimal (and seen only in later stages)[36] (►**Fig. 9**). On MRI, signal alteration with postcontrast enhancement is limited to the anterior aspect of vertebral bodies with loss of anterior vertebral cortical outline.
  Longitudinally extending peripherally enhancing collection is seen deep to the ALL which is seen as an anteriorly displaced T1/T2 hypointense line on sagittal images.[22]
- *Central pattern*: This is seen when infection seeding occurs via Batson's plexus/posterior vertebral artery branches leading to the involvement of the central portion of the vertebral body. Disc involvement and pre-/paravertebral collection are seen only at a later stage in this subtype. It manifests as a focal area of signal alteration within the vertebral body showing postcontrast enhancement which evolves later into a peripherally enhancing intraosseous collection. This pattern of involvement is sometimes difficult to differentiate from neoplastic/metastatic involvement[37] (►**Fig. 10**).
- *Posterior element TB*: This refers to the involvement of pedicles, laminae, transverse, and spinous processes (in isolation or combined); this pattern is rare but more commonly seen in TB compared with pyogenic infection. Posterior elements are usually affected by contiguous extension from vertebral involvement and are rarely involved in isolation[26] (►**Fig. 11**).
- *Cord changes*: More commonly, cord involvement is due to extrinsic mechanical compression by collection, gibbus deformity, or subluxation. Compressive myelopathy is seen as a focal increased T2 signal with maintained bulk in the early stage and cord atrophy/myelomalacia/syrinx formation in later stages (►**Fig. 11**). Less commonly, cord involvement is due to direct involvement where it manifests as multiple small enhancing T2 hypointense nodular

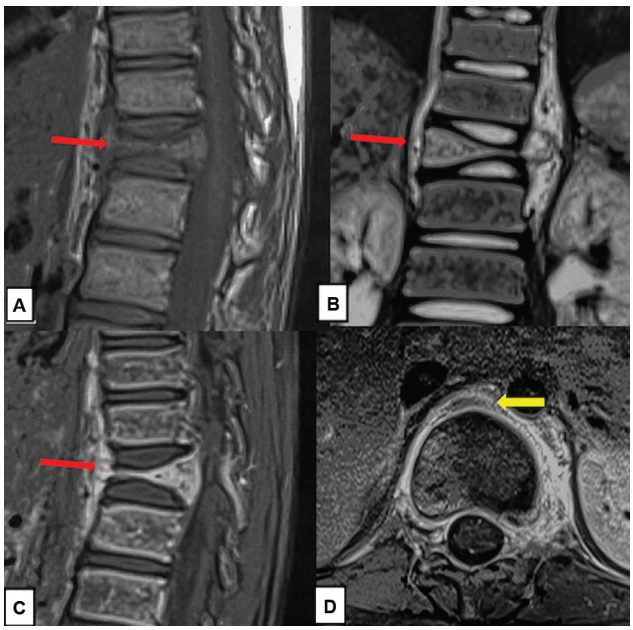

Fig. 10 Central pattern: Sagittal T1-weighted (T1W) non-fat-suppressed (FS) (**A**), coronal T2 FS (**B**), sagittal and axial postcontrast T1 FS (**C** and **D**) show D11 vertebral collapse with abnormal signal and enhancement with preserved intervertebral (IV) discs (red arrows), mild paravertebral soft tissue inflammation on T2. Careful examination of the axial postcontrast image shows a small peripherally enhancing prevertebral collection (yellow arrow) with surrounding inflammation suggesting the diagnosis.

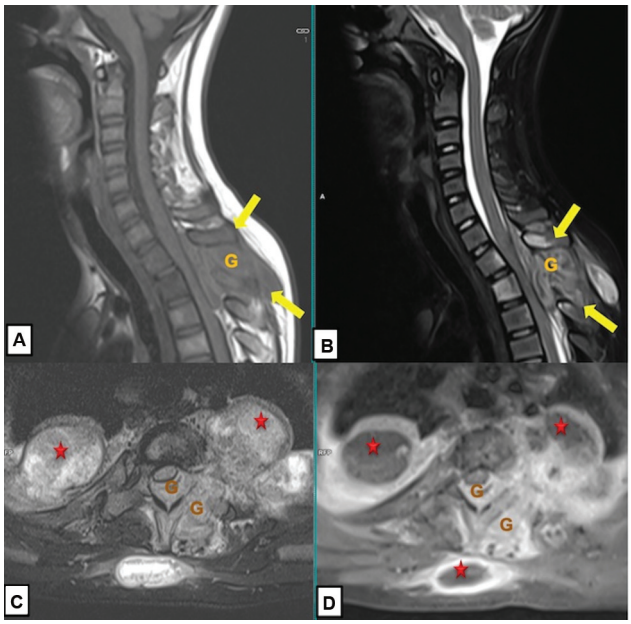

Fig. 11 Posterior element spine tuberculosis (TB). Sagittal T1 non-fat-suppressed (FS) (**A**) and T2 FS (**B**) cervical spine magnetic resonance imaging (MRI) reveals T1 hypointense and T2 hyperintense signal alteration in the D1 and D2 vertebrae, along with involvement of posterior elements and spinous processes (yellow arrows). A heterogeneously T2 hypointense granulation soft tissue (G) is causing separation of the D1 and D2 spinous processes and is extending into the posterior epidural space causing spinal canal compromise, cord compression, and displacement anteriorly along with T2 hyperintense cord signal suggestive of compressive myelopathy. Axial T2 FS and postcontrast T1 FS images (**C** and **D**) show T2 hyperintense signal and abnormal postcontrast enhancement in the left pedicle, lamina, posterior spinous process, and left posterior rib along with left costotransverse joint involvement. Homogenously enhancing granulation tissue (G) and large peripherally enhancing collections (star) in bilateral paravertebral location.

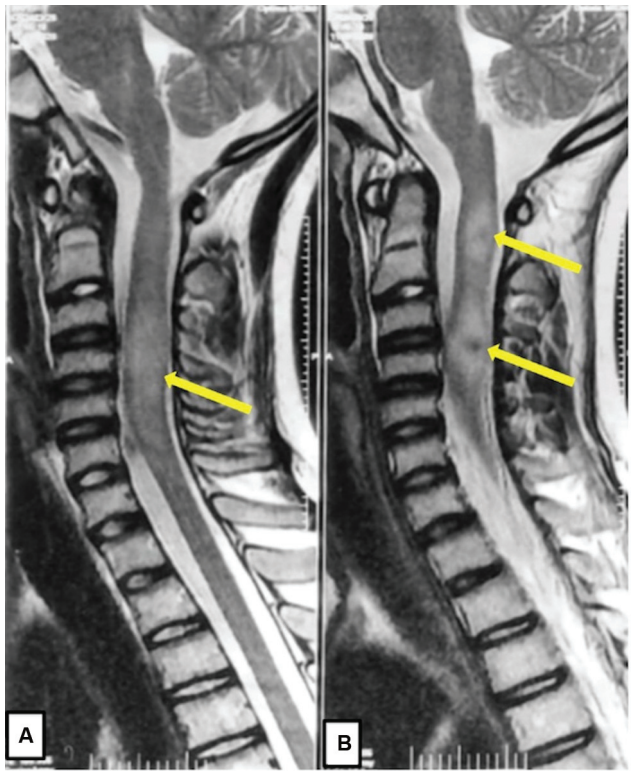

Fig. 12 Tuberculosis (TB) cord involvement: Sagittal T2 cervical spine images (**A** and **B**) showing intramedullary T2 hypointense discrete foci (yellow arrows in **B**) with perilesional edema (yellow arrow in **A**) causing expansion of the cord. The vertebral bodies and intervertebral (IV) discs are normal, and no pre-/paravertebral collection is seen. The patient also had multiple T2 hypointense granulomas in the brain.

intramedullary lesions with or without surrounding edema[36] (►**Fig. 12**).

- *Arachnoiditis*: Occasionally, there is abnormal leptomeningeal enhancement overlying the spinal cord, indicating

Table 1 Key differentiating points among tubercular, pyogenic, and Brucella spondylitis

	Tubercular	Pyogenic	Brucellosis
Clinical presentation	Chronic	Acute	Chronic
Pulmonary TB changes	Old/active changes usually seen	Absent	Absent
Common site of involvement	Thoracolumbar	Lumbar	Lumbar
Vertebral involvement pattern	Long segment (> 3) Heterogeneous enhancement More severe destruction Collapse common	Shorter segment (< 2) Homogenous enhancement Less severe destruction Collapse rare	Less severe destruction Homogenous enhancement Collapse rare Sclerosis in chronic cases
Disc	Preserved till late	Early destruction	Intact until late Air within the disc
Paraspinal collection	Thin and smooth walled	Thick and irregular wall	Minimal, thin walled
Calcification within collection	Common	Rare	May be present
Neural arch involvement	Common	Rare	Rare
Skip lesion	Common	Rare	Rare
Marginal osteophytes	–	–	Present

Abbreviation: TB, tuberculosis.
Note: This table outlines the distinctive clinical, radiological, and laboratory features that help differentiate between spinal tuberculosis from other spinal infections.

Table 2 Distinguishing features of tubercular vertebral involvement compared to metastases and traumatic/osteoporotic collapse

	Tuberculosis	Metastases	Traumatic/Osteoporotic collapse
Vertebral endplate	Irregular/destroyed	Intact	Mostly intact, maybe fractured
Disc	Involved	Spared	Spared
Posterior elements	Usually spared	Involved	May be involved
Collections/sinus tracts	Present	Absent	±Adjacent hematoma
Calcification	Present	Absent	Absent, fractured bony fragments may be seen
Signal alteration on MRI	Usually paradiscal	Involves the whole vertebral body	Linear area limited to the fracture site

Abbreviation: MRI, magnetic resonance imaging.
Note: This table enumerates the key imaging differentiating points between vertebral collapse caused by tubercular etiology and other causes such as metastases and traumatic or osteoporotic collapse.

arachnoiditis. This typically presents as a smooth, thin layer, unlike the irregularity seen in leptomeningeal carcinomatosis. Thickening and clumping of the cauda equina roots may be evident, often accompanied by abnormal enhancement of nerve roots as well. Additionally, arachnoiditis can lead to the formation of CSF loculations, which are extramedullary lesions with clear fluid signal intensity and imperceptible walls. Identifying these lesions is crucial as they may cause cord contour changes and could necessitate surgical intervention. Long-standing arachnoiditis can progress to diffuse myelitis without the presence of focal intramedullary lesions.[38]

Differential Diagnoses

1. Other spinal infections: ►**Table 1** delineates the differentiating points from other spinal infections.[39–41]
2. Metastases or traumatic collapse: ►**Table 2** enumerates the distinguishing points of TB from metastases and traumatic/osteoporotic collapse[42,43] (►**Fig. 13**).
3. Spondyloarthritis: Andersson lesion/sterile spondylodiscitis in ankylosing spondylitis is a discovertebral lesion seen in the late stages of the disease, which may mimic TB spondylodiscitis. However, in this case, background changes of spondyloarthritis will be seen.[44] Fever is typically not associated with these lesions. The findings are seen at the site of the unfused intervertebral disc or the site of fracture in the rigid spine (the last mobile segment) and it usually extends to the neural arch with fracture of the posterior elements as well. There is significant sub-endplate sclerosis. Pre-/paravertebral/epidural collections are not seen in the Andersson lesion.[45]
4. Degenerative spine disease/spondylosis: Rarely, degenerative endplate changes are differential for paradiscal

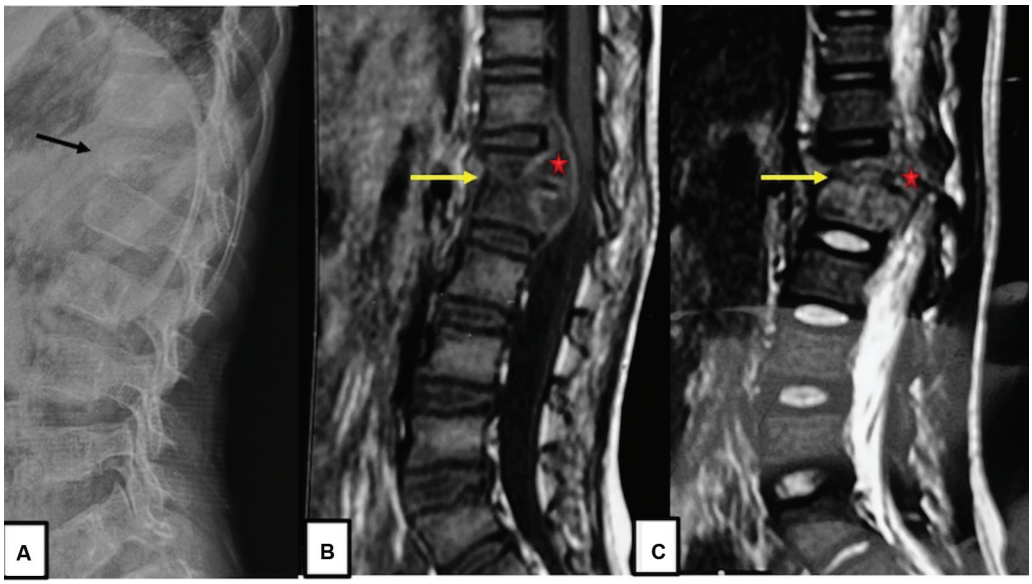

Fig. 13 Magnetic resonance imaging (MRI) solved the radiographic dilemma. Lateral radiograph lumbar spine (**A**) shows collapse of D12 vertebral body (black arrow) in a 5-year-old child with maintained D11–12 and only partial loss of D12–L1 intervertebral (IV) disc space, and a possibility of eosinophilic granuloma was considered. Sagittal T1 non-fat-suppressed (FS) and T2 FS (**B** and **C**) images of MRI done a few weeks after the radiograph reveal paradiscal involvement of D12 and L1 vertebrae with complete obliteration of the intervening IV disc (yellow arrow). T1 hypointense, T2 hyperintense anterior epidural collection (star) contiguous with the posterior aspect of the affected vertebrae seen extending superiorly up to D11 level causing significant spinal canal compromise. Note the T1 hyperintense rim of the collection on noncontrast T1 non-FS sequence suggesting granulation tissue. MRI findings were diagnostic of tuberculosis (TB).

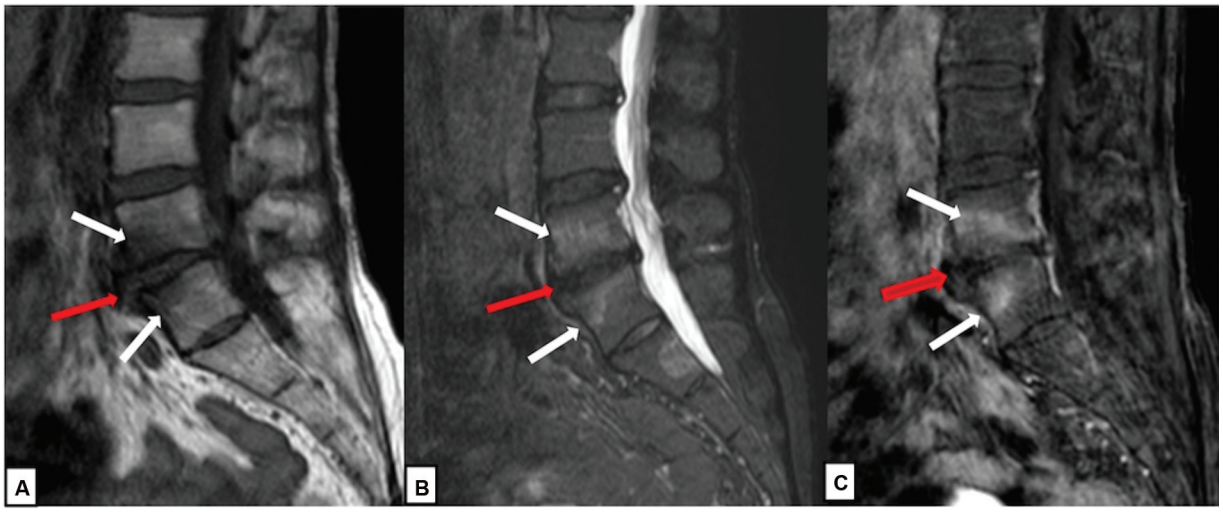

Fig. 14 Type 1 Modic degenerative change. Sagittal T1 non-fat-suppressed (FS) (**A**), T2 FS (**B**), and T1 postcontrast (**C**) magnetic resonance imaging (MRI) images showing sub-endplate vertebral signal alteration in the form of hypointense T1, hyperintense T2 signal, and mild postcontrast enhancement (white arrows). The intervening disc (red arrow) shows reduced height, T2 hypointense signal, and anterior disc bulge. The endplate cortical outline is intact (seen on the T1 image), and enhancement is limited to the periphery of the edema. No pre-/paravertebral collection seen.

involvement of TB. An absence of hyperintensity on T2W image with absent postcontrast enhancement within the disc is critical to make the diagnosis of Modic 1 endplate changes. The endplate lining is irregular but intact in Modic 1 and blurred in spondylodiscitis. The vertebral body shows sub-endplate marrow edema; however, a thin line of sclerosis is seen between the disc and bone edema in degenerative changes[40,45] (►**Fig. 14**).

Rarely, neuropathic spine involvement may simulate TB spine. The presence of gross disorganization (jigsaw spine) along with features of the cause of the disease in the form of syrinx or any traumatic cord pathology may be seen. Preservation of bone density in the neuropathic spine is typical unlike in the tubercular spine. Enhancing soft tissue may be confused with homogeneously enhancing granulation tissue; however, peripherally enhancing collection is not seen in neuropathic involvement.[46]

Other rare differentials for TB spine also include spine involvement in SAPHO (synovitis, acne, pustulosis, hyperostosis, osteitis) syndrome, characterized by a curvilinear or semicircular pattern of contiguous vertebral involvement, distinct from IVD edema and enhancement typically seen in TB. Additionally, dialysis-induced spondyloarthropathy may occasionally pose a diagnostic challenge, but correlation with the duration of hemodialysis, along with the presence of T1/T2 hypointense amyloid deposits and the absence of paravertebral collections, helps clarify the diagnosis.[40]

Extra-spinal Osteoarticular TB

Clinical Presentation

Osteoarticular TB usually presents with chronic pain, swelling, and decreased range of motion of the affected bone or joint. Constitutional symptoms, such as fever, weight loss, and night sweats, may also be present. The onset is insidious, and the disease progression is slow. In advanced cases, cold abscesses and sinus tracts may develop which are important diagnostic clues of TB. The clinical presentation is often nonspecific, leading to delayed diagnosis.[9]

Imaging Features

The imaging features are discussed in ►**Table 3** and vary depending on the stage of pathology[4,6,20,47] (►**Fig. 15**).

TB of Joints

The infection typically starts in the synovium and then extends to the subchondral bone, causing erosions and joint destruction. The hip and knee joints are most commonly affected, followed by the ankle, elbow, and wrist.[48] Tuberculous arthritis is usually monoarticular, as is the case with most infectious joint diseases. Tuberculous arthritis can also occur secondary to tuberculous osteomyelitis, in which a primarily tuberculous metaphyseal focus crosses the epiphyseal plate. This transphyseal spread is one of the hallmarks of tuberculous skeletal infection, not found in pyogenic arthritis. If untreated, infection spreads to para-articular soft tissue to form collections and sinus tracts. *M. tuberculosis* is rarely isolated from these sinus tracts because of frequent pyogenic contamination.[5,49]

Radiography: Early findings include periarticular osteopenia, osseous marginal erosions, and gradual joint space narrowing—Phemister's triad and soft tissue swelling.[50] Calcification within the soft tissue opacity is a strong pointer toward TB (►**Fig. 16**). In advanced stages, severe joint destruction and fibrous ankylosis may occur. Radiological assessment can be done through Kerri and Martini staging classification. This staging classification was described for TB of the knee; however, this can be applied to other joint TB as well.[51]

Table 3 Imaging correlates of pathological features in extraspinal osteoarticular TB

Pathology	Radiograph	MRI
Synovitis: Effusion	Effusion: displacement of periarticular fat pads	Effusion
Granulomatous synovial lesion	–	Synovial thickening (T2 hypointense) and enhancement
Juxta-articular hyperemia	Juxta-articular osteopenia	Subchondral marrow edema
Erosion + cartilage destruction	Gradual decrease in joint space Articular cortex irregularity and erosions	Cartilage destruction, defect in the hypointense articular lining with subchondral bone erosions/intraosseous collection
Para-articular soft tissue masses + cold abscess + sinus tract	Periarticular soft tissue opacity	Para-articular T2 hypointense, homogeneously enhancing granulation tissue/rim enhancing collection, myositis, cellulitis, tenosynovitis, bursitis, and skin ulceration/sinus tract formation
End-stage	Joint deformity, collapse of subarticular bone, sclerosis, fibrous ankylosis	Gross destruction of subchondral bone Fibrous ankylosis: blurry articular cortex line with T1/T2 iso-hypointense signal tissue bridging the bones
Granuloma in bone followed by caseation Extension outside bone to periosteum and soft tissue/adjacent joint	Ill-defined lucent area—focal eccentric geographic lytic lesion with local osteopenia Minimal periosteal reaction ± soft tissue opacity	Focal marrow edema showing enhancement–T1 hypo-, T2/STIR hyperintense peripherally enhancing lesion ± cortical breach ± periosteal thickening/subperiosteal collection ± periosseous collection (more common) Transphyseal spread

Abbreviations: MRI, magnetic resonance imaging; STIR, short tau inversion recovery.
Note: This table highlights the pathological changes associated with extraspinal osteoarticular tuberculosis and their corresponding imaging manifestations on radiographs and MRI. It provides a detailed comparison to help clinicians accurately interpret imaging findings in the context of pathological features.

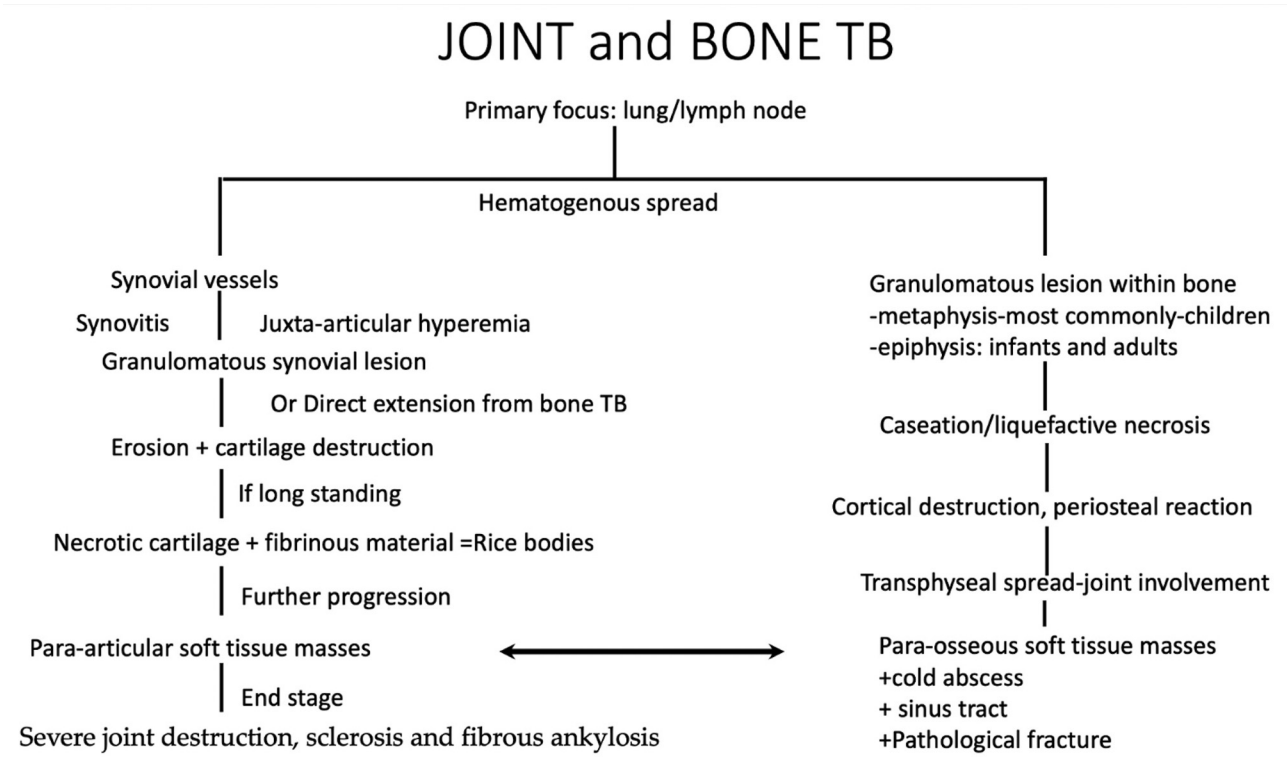

Fig. 15 Joint and bone tuberculosis (TB) pathophysiology.

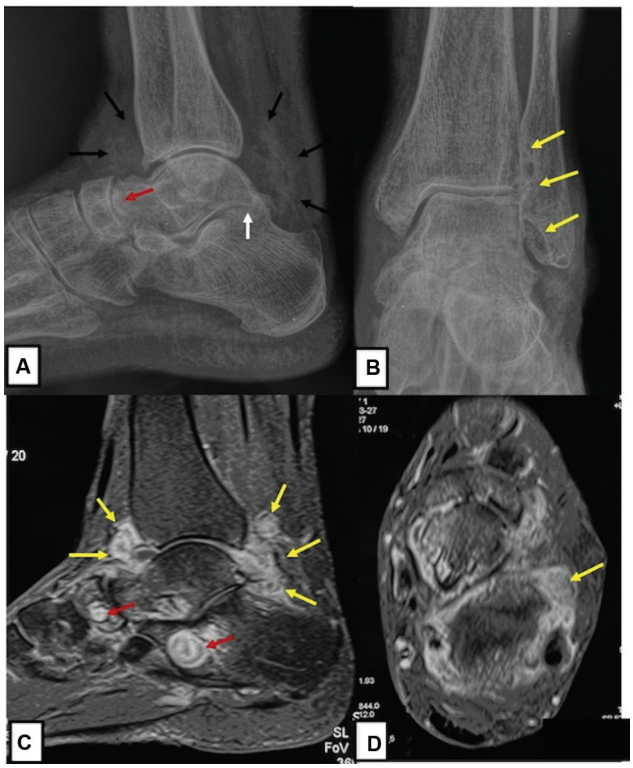

Fig. 16 Tuberculosis (TB) ankle. Radiographs of left ankle lateral (**A**) and anteroposterior (AP) view (**B**) reveal subtle juxta-articular osteoporosis, articular cortex irregularity, and subchondral erosions with reduced joint space (Phemister triad), especially prominent at the talonavicular joint (red arrow), distal tibiofibular and talofibular joint (yellow arrows), as well as the subtalar joint (white arrow). There is replacement of normal fat lucency in the anterior and posterior tibiotalar joint recesses by soft tissue showing dystrophic calcification (black arrows in **A**). Sagittal and axial postcontrast T1 fat-suppressed (FS) images (**C** and **D**) show subchondral erosions with enhancing granulation tissue within (red arrows) and surrounding marrow enhancement, enhancing synovial proliferation (yellow arrows) in the anterior and posterior tibiotalar joint recess.

Stage 1: Localized osteopenia, no erosions, ± soft tissue swelling
Stage 2: One or more osseous erosions, without narrowing of joint space
Stage 3: Narrowing of joint space without gross anatomical disorganization
Stage 4: Narrowing of joint space with gross anatomical disorganization

CT is more sensitive in detecting early bone erosions, sequestrum, and intra-articular loose bodies. Calcification within the periarticular soft tissue can be readily picked up. Its major role is to guide sampling in difficult-to-access areas.[47]

Ultrasound (US) may reveal the presence of synovial proliferation as a hypoechoic nodular thickening showing vascularity, it is not compressible on probe compression (unlike joint effusion that appears anechoic, shows change in shape and internal movement on probe compression, and does not show any vascularity). The role of US is also to provide real-time guidance for joint fluid aspiration or synovial biopsy[11] (►**Fig. 17**).

MRI is the most sensitive modality for detecting early synovial inflammation, bone marrow edema, and subchondral erosions before joint space loss is apparent on X-ray.[5] Synovial thickening with tubercular involvement appears hypointense on T2W images with enhancement on postcontrast images. The T2 hypointensity is attributed to hemorrhage, fibrosis, and inflammatory debris (►**Fig. 18**). Joint effusion appears T2-hyperintense and T1-hypointense without any postcontrast enhancement.[47] MRI can directly assess the articular cartilage damage which is seen as a loss of cartilage thickness with underlying articular cortex erosion. In advanced cases, gross destruction of subchondral bone with intraosseous collection (seen as T1 hypointense, T2 hyperintense lesions showing peripheral enhancement), bone marrow edema and periarticular soft tissue collection, sinus tracts with subluxation or dislocation, and deformity may be seen[52] (►**Fig. 19**). Enlarged regional lymph nodes may be seen, for example, epi-/supratrochlear and axillary in elbow and shoulder, popliteal and inguinal in knee and hip joint infection[48] (►**Fig. 20**).

Differential Diagnosis of TB Arthritis

Pyogenic arthritis: ►**Table 4** compiles the key points in differentiating pyogenic from tuberculous arthritis.[4,5,53]
Rheumatoid arthritis (RA): ►**Table 5** collates the key points in differentiating rheumatoid from tuberculous arthritis.[37,47,54]

RA can mimic tuberculous arthritis, particularly when RA presents with monoarticular involvement. Periarticular osteopenia and joint effusion are seen in both.

Inflammatory sacroiliitis: Distinguishing between inflammatory sacroiliitis as part of axial spondyloarthritis (and tubercular sacroiliitis presents challenges, as both conditions may manifest with subchondral marrow edema, erosions, and capsulitis. The traditional teaching suggests that unilateral involvement indicates an infectious etiology, while bilateral involvement leans toward an inflammatory origin. However, the differentiation becomes complex when there is only unilateral active inflammatory involvement (asymmetrical).

Key indicators of an infective etiology include disproportionate marrow edema, larger erosions, and periarticular collections. Conversely, features suggestive of an inflammatory etiology include the concomitant presence of chronic sacroiliitis features like subchondral sclerosis and fat metaplasia, enthesitis at specific sites, human leukocyte antigen (HLA)-B27 positivity, and signs of spondyloarthritis in the spine.

However, early-stage infective involvement lacking overt erosions and collections may closely resemble early inflammatory involvement. In such cases, the definitive diagnosis often relies on thorough sampling.[40]

Inflammatory seronegative arthritis: Peripheral joint involvement in spondyloarthritis tends to be asymmetric, predominantly affecting the lower extremities rather than the upper extremities. Conditions like reactive arthritis and psoriatic arthritis can mimic tuberculous arthritis when they present with asymmetric oligoarticular involvement.[55]

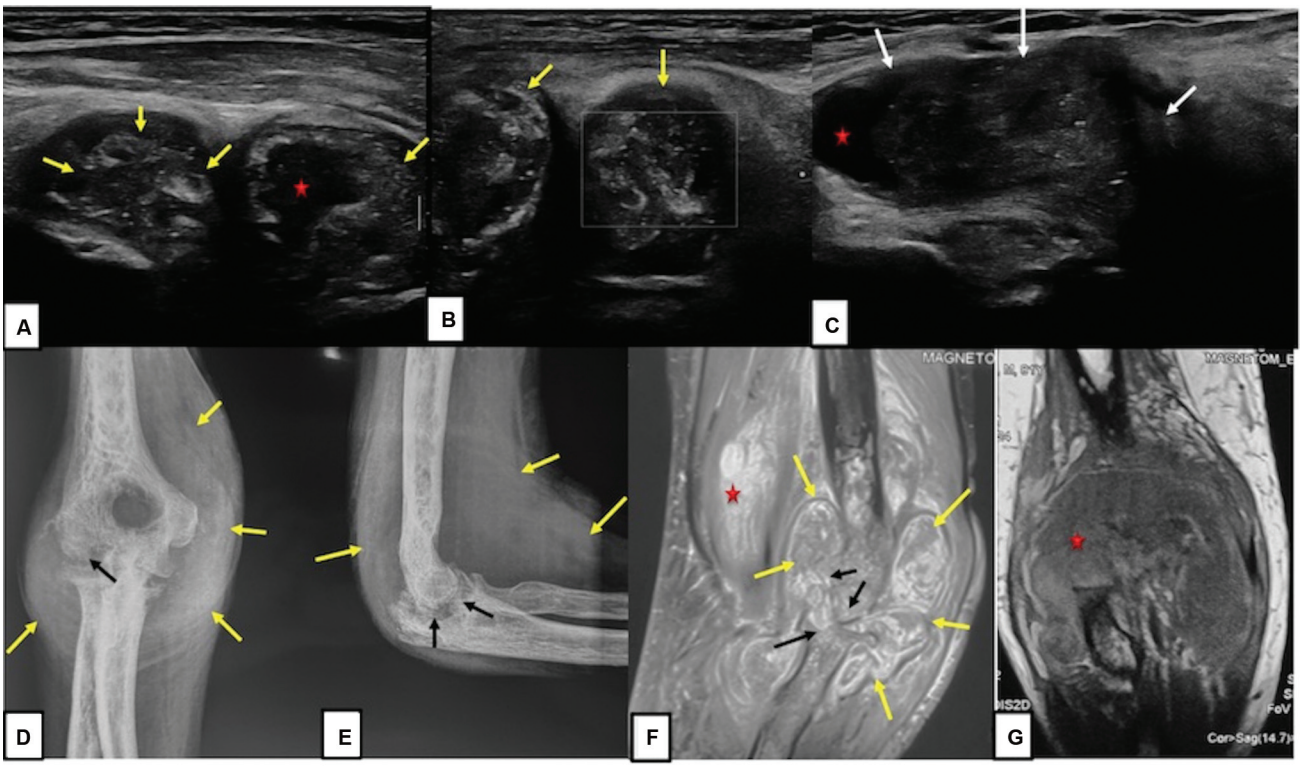

Fig. 17 Role of ultrasound. Longitudinal view with the probe placed along the dorsal radial aspect of the right elbow joint, grayscale (**A**) and color Doppler (**B**), shows heterogeneously hypoechoic synovial proliferation (yellow arrows) with interspersed fluid clefts (star), no significant internal vascularity was seen on Doppler. Longitudinal ultrasound view along the volar aspect (**C**) reveals a large collection (white arrows) with hypoechoic content that showed moving echoes on dynamic compression. Radiographs, anteroposterior (AP) and lateral view (**D** and **E**), show joint space loss with articular margin erosions (black arrows), and periarticular soft tissue prominence (yellow arrows). Sagittal T2 fat-suppressed (FS) and coronal T1 non-FS images (**F** and **G**) show articular margin erosions along the distal humerus and proximal radius (black arrows) with significant marrow edema. Exuberant synovial proliferation appearing T2 hypointense with surrounding hyperintense fluid (yellow arrows) is seen along with a large periarticular collection (star) along the volar aspect of the joint. Note the significant periarticular soft tissue inflammation. The periarticular collection shows a T1 hyperintense rim (penumbra sign).

Additional features such as changes in the axial skeleton (sacroiliitis, syndesmophytes), enthesitis, clinical manifestations like skin and nail changes (in psoriatic arthritis), and symptoms indicating eye/genital involvement (in reactive arthritis), along with elevated HLA-B27 levels, can provide valuable diagnostic clues. Unlike tubercular arthritis, psoriatic joint involvement typically does not result in juxta-articular osteopenia or joint space reduction.[6,37]

Fungal arthritis: Fungal infections of the joints, such as those caused by Aspergillus species, may resemble tuberculous arthritis.[6] However, fungal arthritis is more frequently observed in immunocompromised individuals and often exhibits more pronounced bone destruction and soft tissue extension. In both conditions, synovial proliferation appears T2 hypointense. Classic signs like the "dot in circle" sign should be considered in suspected mycetoma cases.[56]

Neuropathic arthropathy: or Charcot joint, can cause destructive changes in the joints that may resemble tuberculous arthritis. However, neuropathic arthropathy is associated with underlying neurologic disorders, such as diabetes mellitus or syringomyelia, and often shows more pronounced joint destruction and deformity. The bone density is usually preserved.[47]

Tuberculous Osteomyelitis

In children, the metaphysis of long bones is most commonly affected due to its rich blood supply. In adults, the vertebrae, pelvis, and large joints are more frequently involved.[49] TB arthropathy is a more common manifestation of osteoarticular TB than TB osteomyelitis.[20] Isolated tubercular osteomyelitis without adjacent arthropathy usually occurs in the long bones (femur and tibia most commonly) and the small bones of the hand and feet.[5]

Early findings on radiography include focal osteopenia, cortical thinning, and periosteal reaction. As the disease progresses, well-defined osteolytic lesions may be seen. Sequestrum formation is less common and less extensive compared with pyogenic osteomyelitis (►**Fig. 21**). In advanced cases, pathological fractures, joint involvement, and development of medullary infarcts due to TB vasculitis may occur.[57]

CT is more sensitive in detecting early bone destruction and sequestrum formation. CT can also guide percutaneous biopsy for microbiological and histopathological diagnosis.

MRI is the most sensitive modality for detecting early marrow changes, soft tissue involvement, and adjacent joint involvement. Marrow changes appear as T1 hypointense and T2 hyperintense lesions, with enhancement on postcontrast images (►**Fig. 22**). An intraosseous collection is seen as T1

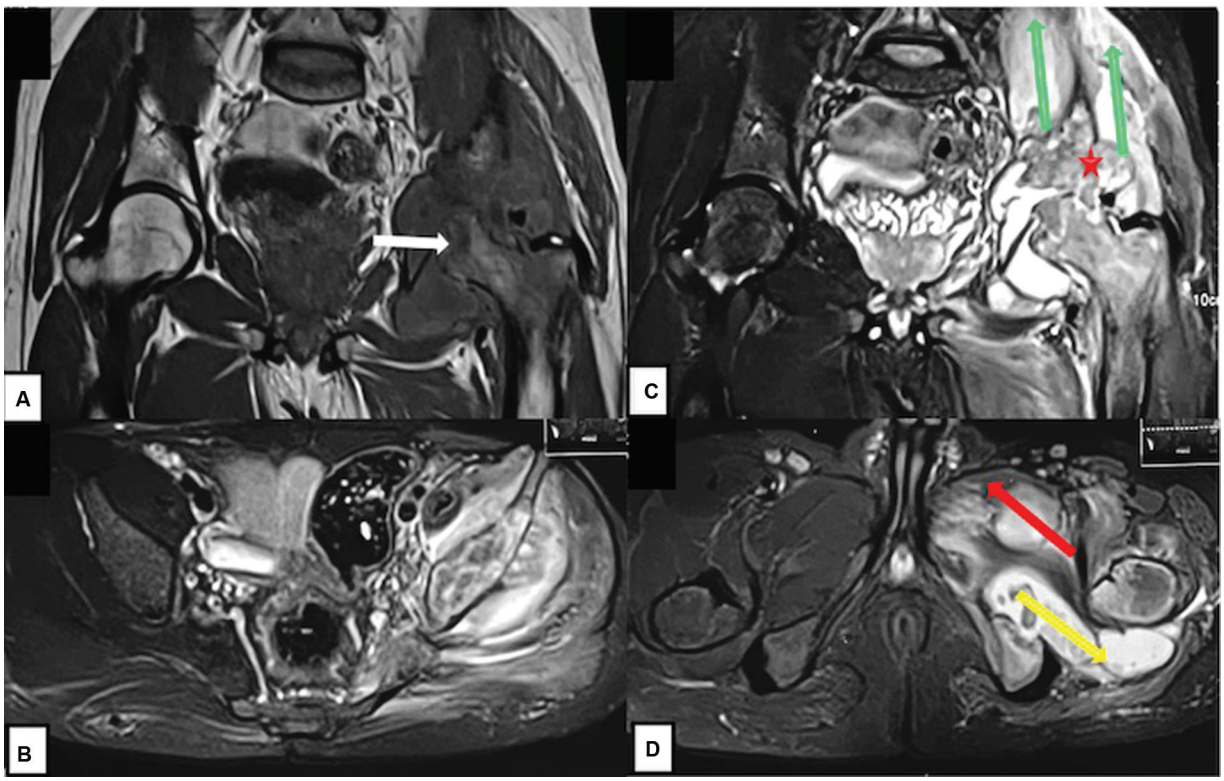

Fig. 18 Tuberculosis (TB) hip. T1 non-fat-suppressed (FS) coronal (**A**), T2 FS coronal, and axial images (**B–D**) show gross subchondral bone destruction (white arrow) and marrow edema involving the acetabular as well as the femoral aspect of the left hip joint with T2 hypointense marked synovial proliferation (star). Periarticular collection and inflammation tracking: superiorly along iliopsoas and gluteus muscles (green arrow), posteroinferiorly along ischiofemoral space (yellow arrow), anteriorly along the adductors (red arrow).

hypointense, and T2 hyperintense with peripheral enhancement. A thin rim of T1 hyperintensity lining the collection may also be seen (penumbra sign), this sign is also seen in periarticular collections (►**Fig. 16**). MRI features of tubercular osteomyelitis are nonspecific and are usually not useful in

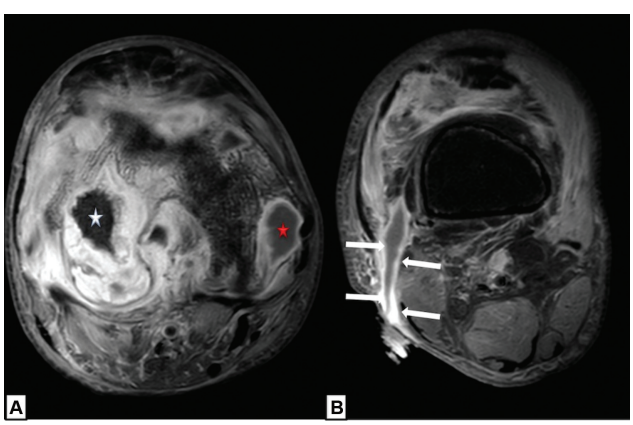

Fig. 19 Tuberculosis (TB) knee with a sinus tract. T1 postcontrast axial magnetic resonance imaging (MRI) images (**A** and **B**) showing a focal nonenhancing bone (B) surrounded by homogenously enhancing soft tissue and bone marrow edema in the lateral femoral condyle s/o sequestrum formation with surrounding granulation tissue (seen in **A**), a peripherally enhancing collection is seen along the medial aspect of the joint s/o collection formation (star in **A**). A sinus tract lined by enhancing granulation tissue extending from the joint to the skin surface is seen in a slightly cranial section (white arrows in **B**).

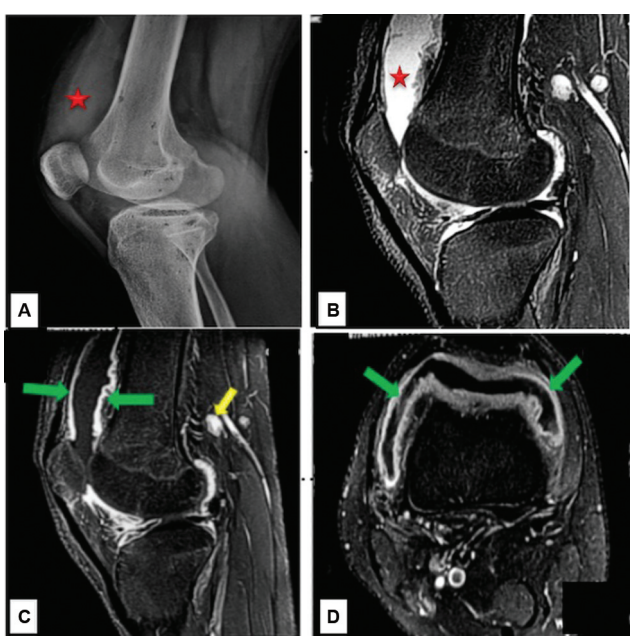

Fig. 20 Tuberculosis (TB) knee synovitis. Radiograph knee lateral view (**A**) reveals loss of normal posterior fat plane of quadriceps tendon suggestive of fluid in suprapatellar recess (star), T2 fat-suppressed (FS) sagittal (**B**) and T1 postcontrast sagittal and axial magnetic resonance imaging (MRI) image (**C** and **D**) shows T2 hyperintense joint fluid in suprapatellar recess (star) and uniform synovial thickening and enhancement (green arrows), few enlarged popliteal lymph nodes are also seen (yellow arrow).

Table 4 Key points for differentiating pyogenic arthritis from tuberculous arthritis

	Pyogenic arthritis	Tubercular arthritis
Clinical presentation	Acute toxic	Chronic
Synovial proliferation on MRI	Intermediate to bright signal on T2W	T2 Hypointense
Joint space reduction	Greater degree with early cartilage destruction	Gradual loss
Cartilage loss distribution	Nearly uniform	Uneven
Intraosseous and periarticular collections	Irregular shaggy margin–ill marginated	Smooth thin wall–well marginated
Cellulitis and fasciitis	Extensive	Less severe
Chronic sequelae	Bony ankylosis	Fibrous ankylosis

Abbreviations: MRI, magnetic resonance imaging; T2W, T2-weighted.
Note: This table compiles the essential distinguishing features between pyogenic arthritis and tuberculous arthritis. It includes differences in clinical presentation, imaging findings, laboratory results, and typical disease progression to aid in accurate diagnosis.

differentiating from pyogenic osteomyelitis without appropriate clinical information.[6]

TB Dactylitis

TB dactylitis, also known as spina ventosa, is a form of tuberculous osteomyelitis affecting the short tubular bones of the hands and feet. It is more common in children and presents with diffuse swelling and pain of the affected digit. The radiograph shows expansile, lytic lesions with thinned-out cortex. Minimal periosteal reaction and absence of sequestrum formation differentiate it from pyogenic infections.[58]

Differential Diagnosis of TB Osteomyelitis

The differential diagnosis of tuberculous osteomyelitis includes pyogenic and fungal osteomyelitis, Brodie's abscess, Langerhans cell histiocytosis, and primary bone tumors. Pyogenic osteomyelitis usually has a more acute onset and more pronounced periosteal reaction compared with tuberculous osteomyelitis.

Transphyseal spread of the infection to the joint is one of the hallmarks of TB; though joint space is relatively preserved in early TB infection. Brodie's abscess appears as a well-defined, centrally located osteolytic lesion with a sclerotic rim. Langerhans cell histiocytosis may present with multiple osteolytic lesions and pathological fractures. Primary bone tumors, such as Ewing's sarcoma, may mimic tuberculous osteomyelitis, especially in the early stages.[8]

Giant cell tumor (GCT) and enchondroma of the small bones may mimic tubercular dactylitis. GCT is rare in small bones of hands and feet, it lacks periosteal reaction, and shows a T2 hypointense signal with the absence of surrounding soft tissue inflammation on MRI. Enchondroma is a common benign bone tumor involving the small bones of hands and feet. Enchondroma rarely presents with pain and does not show periosteal reaction unless complicated by a pathological fracture. It does not show surrounding soft tissue inflammation, rather shows rings and arcs (chondroid matrix) pattern calcification.[59]

Table 5 Points for differentiating tuberculous arthritis from rheumatoid arthritis

	Rheumatoid arthritis	Tubercular arthritis
Disease distribution	B/L symmetrical Polyarticular Small joints of the hands and feet	Unilateral Monoarticular Large joints (hip and knee) more commonly
Synovial proliferation: degree and distribution within the joint	More extensive, thickness usually >1 cm Nonuniform distribution within the joint	Relatively thin Uniform proliferation
Erosions	Marginal Numerous Smaller	Nonmarginal More destructive Larger
Cartilage loss	Always before erosions (except at bare area)	Erosions may occur even without cartilage destruction
Extra-articular (cold collections abscesses)	Absent	Usually present
Periarticular bursal/tenosynovial inflammation	More extensive	Less extensive

Note: This table collates the critical distinguishing features between tuberculous arthritis and its close imaging mimic, rheumatoid arthritis.

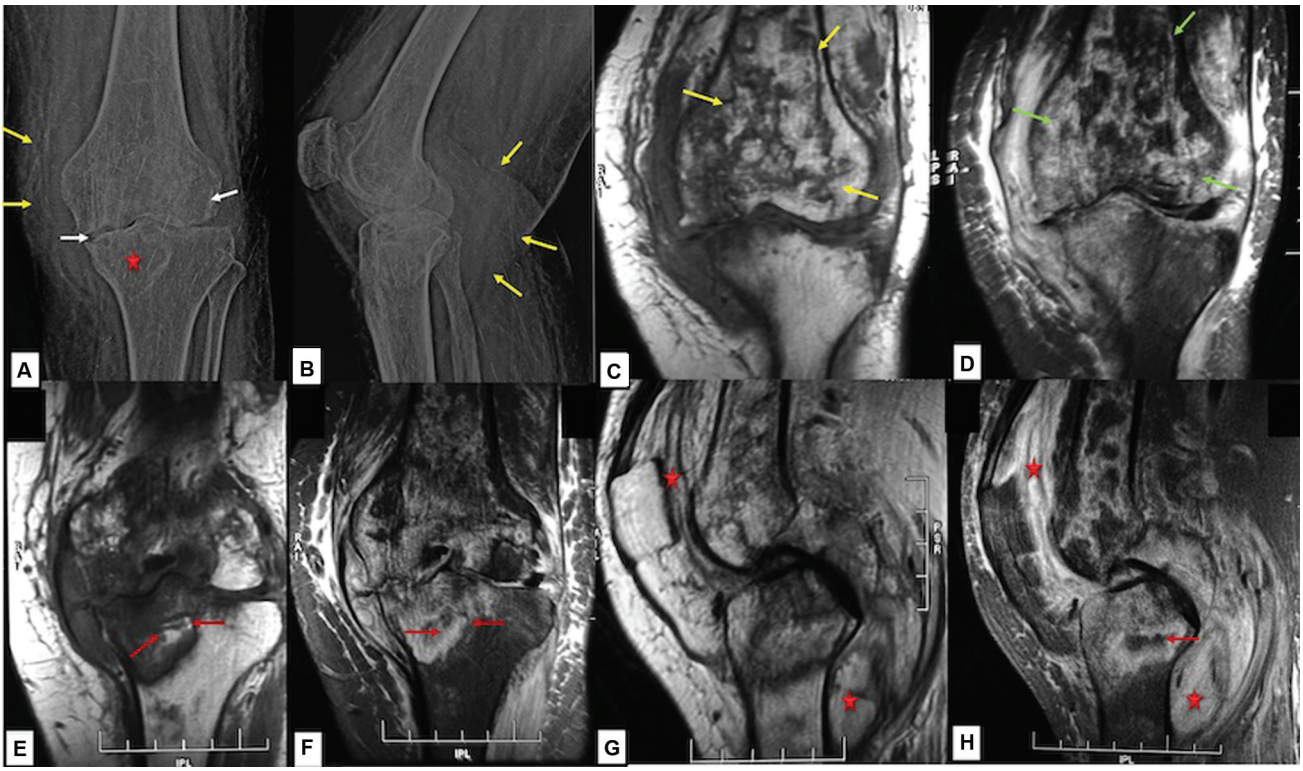

Fig. 21 Tuberculosis (TB) knee complication—sequestrum formation and medullary bone infarct. Radiograph knee anteroposterior (AP) and lateral view (**A** and **B**) reveal reduced tibiofemoral joint space and subchondral erosions (white arrows), mixed lytic-sclerotic lesion in the medial tibial plateau (star), medial and posterior soft tissue prominence (yellow arrows). Coronal T1 non-fat-suppressed (FS) and short tau inversion recovery (STIR), anterior (**C** and **D**) and posterior sections (**E** and **F**), sagittal T2 non-FS and T2 FS (**G** and **H**) show geographic T1 hyperintense, STIR hypointense areas lined by serpiginous outer T1 hypointense and inner STIR hyperintense rim suggestive of medullary infarcts in the distal femur (green arrows in **C** and **D**), markedly T1 hypointense, STIR hyperintense area in medial tibial plateau with a small T1 hyperintense, STIR hypointense focus within (red arrows in **E** and **F**) suggestive of sequestrum with surrounding granulation tissue, minimal fluid with thickened inflamed synovium along with T2 hyperintense collections in posterior periarticular soft tissue (star in **G** and **H**) . Note the significant marrow edema and surrounding soft tissue edema.

Tuberculosis of the Soft Tissues

Tuberculous Tenosynovitis and Bursitis

Tuberculous tenosynovitis and bursitis usually result from direct extension of adjacent osteoarticular TB, or less commonly, from hematogenous spread. The flexor tendons of the hand and wrist are most frequently affected. TB bursitis most commonly involves the greater trochanteric and subacromial bursae.

Calcifications within the soft tissue swelling are highly suggestive of TB.[60] US demonstrates thickening of the tendon sheath or bursal wall, with increased vascularity on color Doppler and fluid within the sheath/bursa. Rice bodies, appearing as linear echogenic foci or round isoechoic

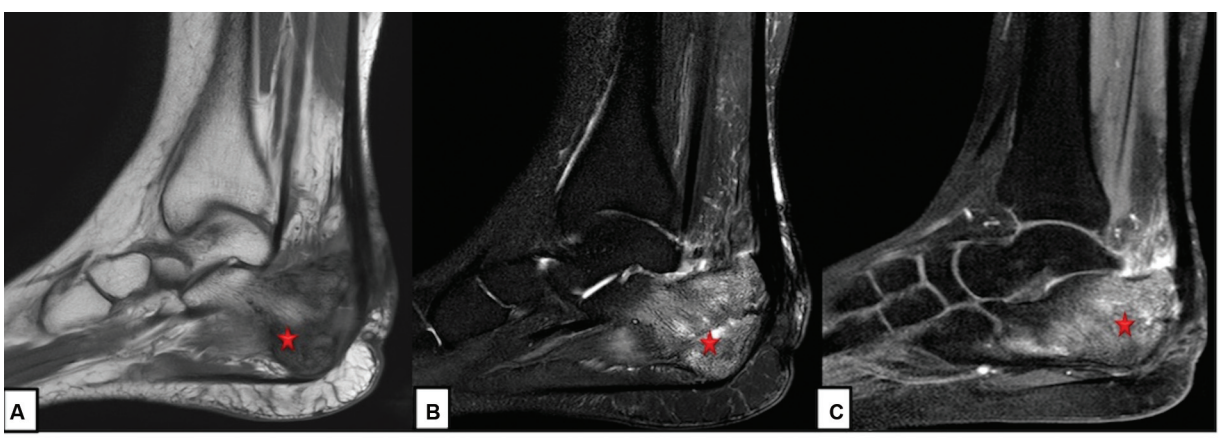

Fig. 22 Tuberculosis (TB) calcaneum: T1 non-fat-suppressed (FS) (**A**), short tau inversion recovery (STIR) (**B**), and postcontrast T1 FS (**C**) showing T1 hypointense, STIR hyperintense signal, and postcontrast enhancement involving the body of the calcaneum (star) with surrounding soft tissue edema.

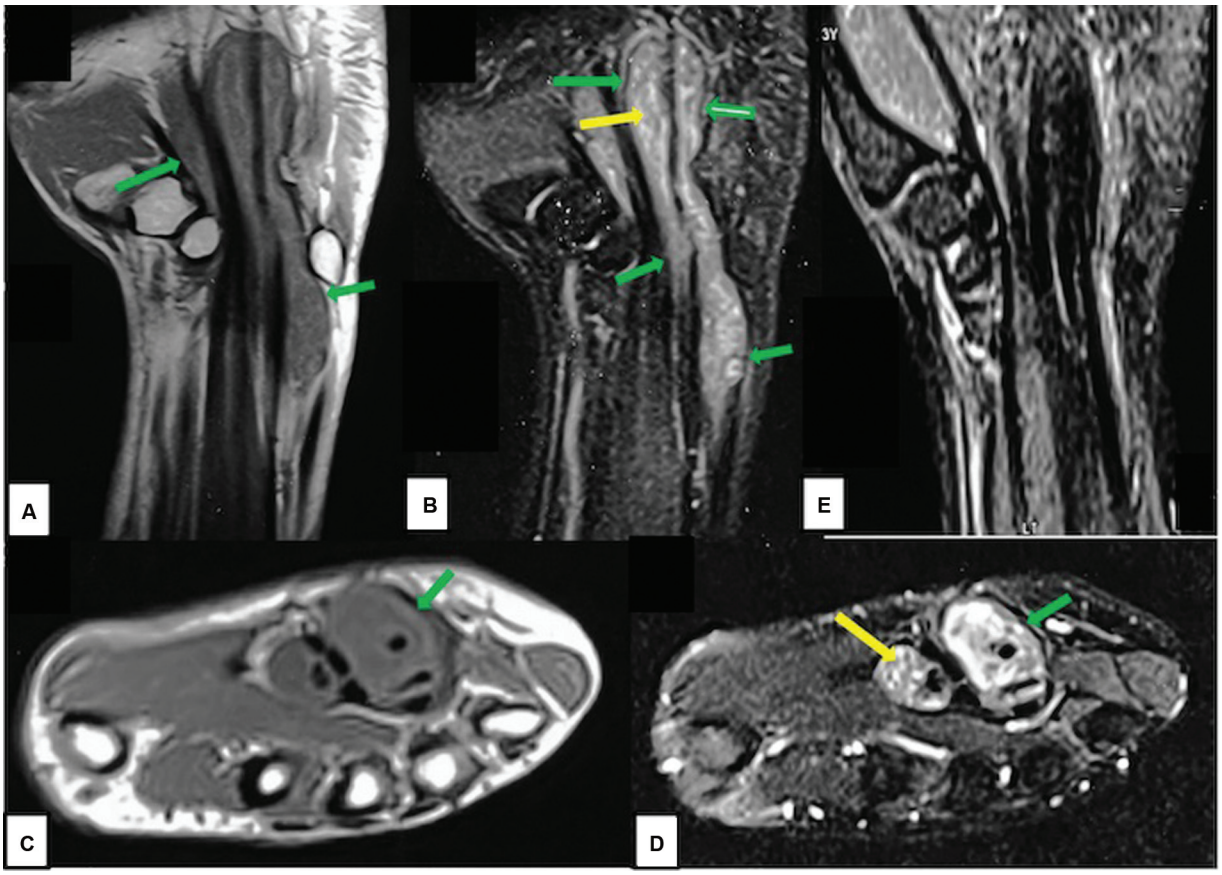

Fig. 23 Tuberculosis (TB) tenosynovitis (compound palmar ganglion). Coronal T1 non- fat-suppressed (FS) and T2 FS (**A** and **B**) and axial T1 non-FS and T2 FS (**C** and **D**) at the level of the wrist volar aspect: An hour-glass shaped mixed signal intensity lesion longitudinally extending along the length of the flexor tendons at the level of the wrist and further into the palm (green arrows). Multiple T2 hypointense foci within the fluid-rice bodies (yellow arrow). Coronal T2 FS image of the same patient (**E**) after completion of antitubercular therapy (ATT) shows complete resolution of the findings.

melon-seed bodies, may be seen within the synovial fluid. US can also guide percutaneous biopsy or aspiration.[47]

MRI is the most sensitive modality for assessing the extent of tenosynovitis and bursitis. The affected tendon sheath or bursal wall along with the synovial lining appears thickened and shows T2 hypointensity and enhancement on postcontrast images. Rice bodies appear as T2 hypointense linear foci within the hyperintense synovial fluid (►**Fig. 23**) and do not show contrast enhancement. MRI can also detect adjacent bone and joint involvement.[61]

The differential diagnosis of tuberculous tenosynovitis and bursitis includes pyogenic infection, RA, and pigmented villonodular synovitis. Pyogenic infection usually has a more acute onset and may show more pronounced peritendinous edema and fluid collections. RA typically involves multiple tendon sheaths and bursae and may show erosions and tenosynovial cysts. Pigmented villonodular synovitis demonstrates characteristic blooming artifacts on gradient-echo sequences due to hemosiderin deposition, it is characteristically located in relationship to the flexor and extensor tendon sheaths of hand.[37]

Tuberculous Myositis

Tuberculous myositis and collection formation are rare and usually result from contiguous spread of adjacent osteoarticular or lymph node TB. The psoas and gluteal muscles are most frequently involved. These collections present as painless, fluctuant masses that may eventually drain to the skin surface, forming sinus tracts.[62]

CT demonstrates a focal or diffuse enlargement of the affected muscle, with hypodense areas suggesting necrosis or collection formation. CT can also detect adjacent bone or joint involvement.

MRI is the most sensitive modality for assessing the extent of myositis and collection formation and ruling out underlying bone involvement. The affected muscle appears enlarged and shows intrasubstance T2 hyperintensity and heterogeneous enhancement on postcontrast images. Collection shows peripheral rim enhancement. MRI can also detect adjacent bone, joint, or lymph node involvement.[5]

The differential diagnosis of tuberculous myositis and collection includes pyogenic infection, sarcoidosis, and soft tissue tumors. Pyogenic myositis and collection usually have a more acute onset and may show more pronounced inflammatory changes on imaging. Sarcoidosis may present with multiple, noncaseating granulomas in the muscles and other organs. Soft tissue tumors, such as sarcomas and lymphomas, may mimic tuberculous myositis, especially in the early stages.[5,6]

Treatment Principles

1. Sampling: All patients with radiological findings suggestive of TB usually undergo image-guided sampling (CT- or US-guided) for microbiological/histopathological confirmation and susceptibility testing except in cases where the site of sampling is not accessible. Whenever possible, both affected bone and soft tissue collection should be sampled. Obtained sample must be sent for AFB staining, NAAT, mycobacterial and bacterial culture, and histopathological examination.
2. Drug therapy: The cornerstone of treatment for musculoskeletal TB is antituberculous chemotherapy (ATT). The standard regimen consists of a four-drug combination of isoniazid, rifampicin, pyrazinamide, and ethambutol.

For drug-susceptible spinal and extraspinal skeletal TB, the following ATT regimen is suggested by the INDEX-TB (Indian Extra-Pulmonary TB) guidelines[63]:

2HRZE (intensive phase) plus 10HRE (continuation phase) for a total of 12 months (extendable to 18 months on a case-to-case basis). Immobilization of the affected joint or limb is important to prevent further joint damage and promote healing. Physical therapy and rehabilitation are essential to maintain joint mobility, prevent contractures, and restore function. Indications for surgery in spine TB include: severe neurological deficits, rapid onset or painful paraplegia, mechanical instability of the spine, and spinal deformity.[19]

In cases of extraspinal TB, surgical interventions such as synovectomy and joint debridement may be warranted in early-stage disease with poor response to nonoperative treatments. Joint debridement and collection drainage can help to reduce the bacterial load and prevent further joint damage. Advanced arthritis may necessitate procedures such as arthrolysis, excision arthroplasty, arthrodesis, or total joint replacement. Additionally, corrective surgeries for deformities resulting from healed disease and drainage of large collections may also be required.

Posttreatment Changes

On radiographs (►**Figs. 24** and **25**):

1. Sharpening of the earlier irregular endplate margins or articular cortex lining

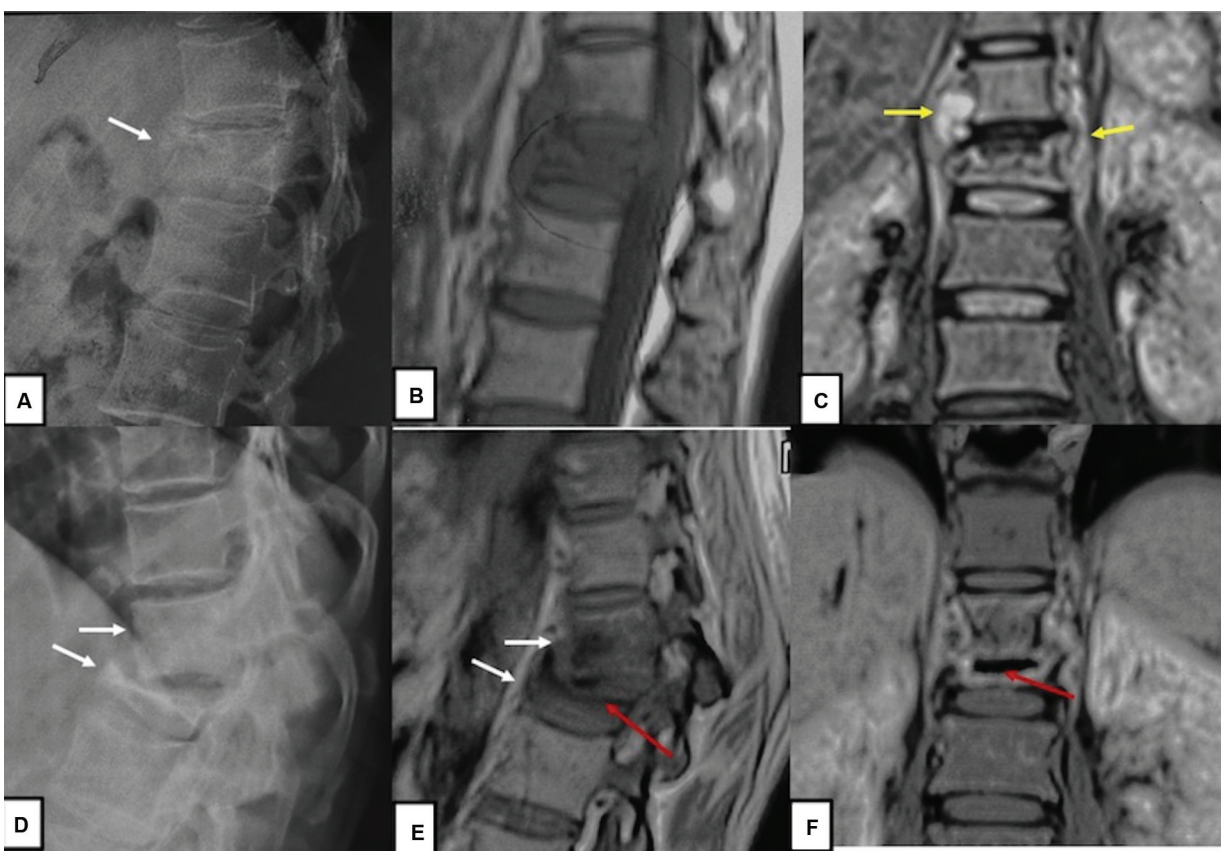

Fig. 24 Signs of healing—sclerosis. Pretreatment radiograph, sagittal T1 non-fat-suppressed (FS) and coronal short tau inversion recovery (STIR) (**A**–**C**). Radiograph reveals decreased overall bone density, wedge collapse of D12 vertebral body, irregular upper endplate with decreased D11/12 intervertebral (IV) disc space (arrows). Magnetic resonance imaging (MRI) shows T1 hypointense and T2 subtle hyperintense signal within the partially collapsed D12 vertebral body and the anteroinferior sub-endplate portion of the D11 vertebral body with endplate irregularity, the intervening disc height is reduced. Small prevertebral as well as bilateral paravertebral collection (R > L) (yellow arrows). Posttreatment radiograph (**D**), sagittal T1 non-FS (**E**), and coronal postcontrast T1 FS (**F**). Radiograph reveals restored bone density, complete collapse of D12 causing mild focal kyphosis, and sclerosis of D11 and D12 (white arrows) with complete loss of D11/12 intervening IV disc space (black arrow). The corresponding changes on MRI are seen as a hypointense signal in D11 and D12 vertebrae (white arrows), markedly hypointense signal suggesting increased sclerosis along the superior margin of collapsed D12 (red arrow), absent contrast enhancement, and complete resolution of the paravertebral collection.

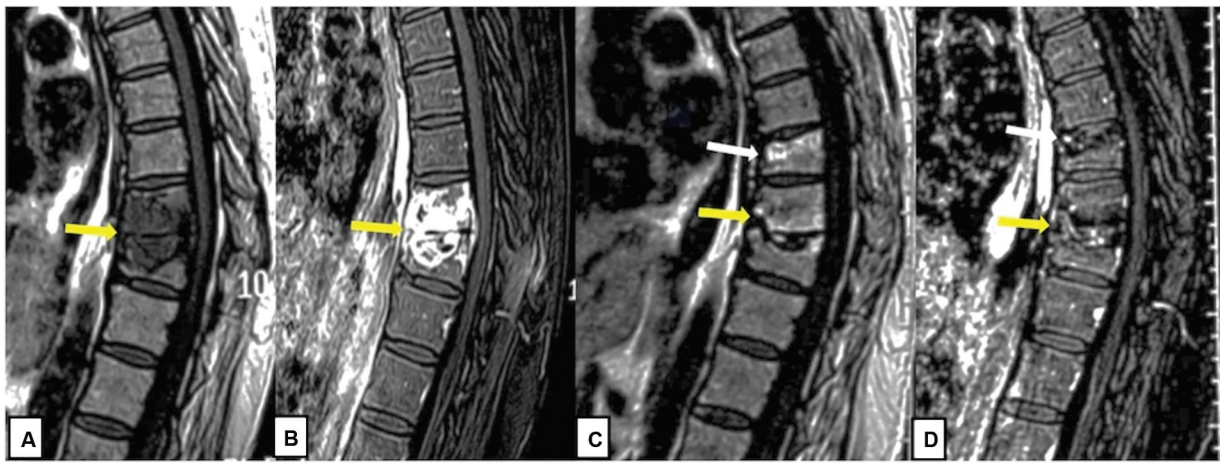

Fig. 25 Signs of healing—fatty marrow infiltration. Baseline sagittal T1 non-fat-suppressed (FS) (**A**), postcontrast T1 FS (**B**) dorsal spine magnetic resonance imaging (MRI) images showing paradiscal involvement of two contiguous vertebral bodies (D9 and D10) and the intervening disc with mild vertebral collapse and small epidural component causing mild focal kyphotic deformity (yellow arrows). The patient received antitubercular therapy (ATT), however, showed clinical worsening and progression on imaging with persistent active disease at D9/10 with new involvement of D8 vertebral body and paravertebral collection. The collection was sampled which showed multidrug-resistant (MDR) tuberculosis (TB). Post-modified MDR TB regimen completion: sagittal T1 non-FS (**C**) and postcontrast T1 FS (**D**) dorsal spine of the same patient showing T1 hyperintense signal within the D9 and D10 vertebrae (yellow arrow) as well as in D8 vertebral body (white arrow) suggestive of fatty replacement and absent contrast enhancement suggestive of complete resolution. The mild kyphotic deformity is persistent. No pre-/paravertebral collection seen.

2. Increase in density/sclerosis of the affected bone suggesting remineralization of the resorbed trabeculae
3. Reduction of IVD space or joint space with ankylosis[29]

On MRI:

1. A decrease in the size of the paraspinal soft issue is the earliest sign of healing.
   The other features of healing include:
2. Fat infiltration (T1 hyperintense signal) at the rim of the osseous lesion
3. Reduction in T2/STIR hyperintensity and enhancement within the bone and IVD space/joint space.
4. Resolution of the intra0/extraosseous collections

Mildly altered signal intensity may persist even after successful treatment. Similarly, thin peripheral contrast enhancement may persist and denote sterile collection.[29]

Response Assessment

Close monitoring of patients during treatment is crucial to assess response to therapy, detect drug toxicity, and identify complications early. Assessing treatment response is best achieved with contrast-enhanced MRI of the spine performed upon completion of ATT, typically at the 12-month mark before termination of therapy. Comparison with prior baseline imaging is essential. Earlier imaging may be warranted if there is suspicion of poor treatment response.[64]

Drug resistance is suspected in patients on ATT for 5 months or more showing poor clinical and radiological response, the appearance of new lesions, worsening of spinal deformity, or wound dehiscence of previously operated scar. It is imperative to verify drug compliance before assigning a drug-resistant label.

In cases with partial response with persistent active disease, ATT is prolonged for an additional 6 months, with a follow-up contrast-enhanced MRI of the spine at 18 months. Sometimes, sampling of new lesions may be necessary to detect the emergence of resistant strains in a previously drug-sensitive TB particularly in patients that were initially started on ATT on a clinicoradiological basis without microbiological confirmation.

The final decision of termination of ATT is taken considering both radiological as well as clinical response. The clinical response encompasses symptom resolution, normalization of laboratory parameters (erythrocyte sedimentation rate/C-reactive protein), and clinical signs.[65]

Conclusion

Imaging assumes a pivotal role in the evaluation of musculoskeletal TB. Despite adequate sampling, histopathological or microbiological testing may fail to yield the organism owing to the paucibacillary nature of the disease. Hence, patients displaying classical findings on imaging are often started empirically on ATT. Furthermore, imaging not only aids in diagnosis but also guides sampling, assesses treatment response, detects complications, and helps make decisions regarding therapy termination. Thus, it serves as a comprehensive tool throughout the management of musculoskeletal TB.

Learning Points

1. Contrast-enhanced MRI is the preferred imaging modality for diagnosing and assessing response in both spinal and extraspinal TB.

2. TB-related synovial proliferation typically appears T2 hypointense.
3. US plays a significant role in assessing superficial joints and soft tissues and guides sampling for diagnosis.
4. Calcification within paraspinal or periarticular soft tissue collections strongly suggests TB.
5. Early posttreatment imaging is discouraged unless there is clinical nonresponse, as it may falsely suggest progression and lead to unnecessary interventions. Response assessment imaging should be conducted near treatment completion.
6. Mild residual osteoarticular enhancement and stable paraspinal or periarticular collections (with thin rim enhancement) may persist and do not indicate treatment failure. In an appropriate clinical context, it may be prudent to stop therapy even when mild residual enhancement persists and repeat the imaging after a few months to document healed disease.

Funding
None.

Conflict of Interest
None declared.

References

1 Xue Y, Zhou J, Wang P, et al. Burden of tuberculosis and its association with socio-economic development status in 204 countries and territories, 1990-2019. Front Med (Lausanne) 2022;9:905245
2 Global Tuberculosis Report 2022. Accessed April 17, 2024 at: https://www.who.int/teams/global-tuberculosis-programme/tbreports/global-tuberculosis-report-2022
3 Sharma SK, Mohan A, Kohli M. Extrapulmonary tuberculosis. Expert Rev Respir Med 2021;15(07):931–948
4 Watts HG, Lifeso RM. Tuberculosis of bones and joints. J Bone Joint Surg Am 1996;78(02):288–298
5 De Vuyst D, Vanhoenacker F, Gielen J, Bernaerts A, De Schepper AM. Imaging features of musculoskeletal tuberculosis. Eur Radiol 2003;13(08):1809–1819
6 De Backer AI, Mortelé KJ, Vanhoenacker FM, Parizel PM. Imaging of extraspinal musculoskeletal tuberculosis. Eur J Radiol 2006;57 (01):119–130
7 Jain AK. Tuberculosis of the spine: a fresh look at an old disease. J Bone Joint Surg Br 2010;92(07):905–913
8 Gardam M, Lim S. Mycobacterial osteomyelitis and arthritis. Infect Dis Clin North Am 2005;19(04):819–830
9 García-Rodríguez JF, Álvarez-Díaz H, Lorenzo-García MV, Mariño-Callejo A, Fernández-Rial Á, Sesma-Sánchez P. Extrapulmonary tuberculosis: epidemiology and risk factors. Enferm Infecc Microbiol Clin 2011;29(07):502–509
10 Caulfield AJ, Wengenack NL. Diagnosis of active tuberculosis disease: From microscopy to molecular techniques. J Clin Tuberc Other Mycobact Dis 2016;4:33–43
11 Gopalaswamy R, Dusthackeer VNA, Kannayan S, Subbian S. Extrapulmonary tuberculosis—an update on the diagnosis, treatment and drug resistance. J Respir. 2021;1(02):141–164
12 Rao PD, Devi DRG, Gouri SRM, Arjun AS, Krishnappa L, Azeem A. Evaluation of immunohistochemistry technique for diagnosis of extrapulmonary tuberculosis in biopsy tissue specimen as compared to composite diagnostic criteria. J Glob Infect Dis 2022;14 (04):136–141
13 Allali F, Mahfoud-Filali S, Hajjaj-Hassouni N. Lymphocytic joint fluid in tuberculous arthritis. A review of 30 cases. Joint Bone Spine 2005;72(04):319–321
14 Mekkaoui L, Hallin M, Mouchet F, et al. Performance of Xpert MTB/RIF Ultra for diagnosis of pulmonary and extra-pulmonary tuberculosis, one year of use in a multi-centric hospital laboratory in Brussels, Belgium. PLoS One 2021;16(04):e0249734
15 Rindi L. Rapid molecular diagnosis of extra-pulmonary tuberculosis by Xpert/RIF Ultra. Front Microbiol 2022;13:817661
16 Sun Q, Wang S, Dong W, et al. Diagnostic value of Xpert MTB/RIF Ultra for osteoarticular tuberculosis. J Infect 2019;79(02): 153–158
17 Rasouli MR, Mirkoohi M, Vaccaro AR, Yarandi KK, Rahimi-Movaghar V. Spinal tuberculosis: diagnosis and management. Asian Spine J 2012;6(04):294–308
18 Agrawal V, Patgaonkar PR, Nagariya SP. Tuberculosis of spine. J Craniovertebr Junction Spine 2010;1(02):74–85
19 Rajasekaran S, Kanna RM, Shetty AP. Pathophysiology and treatment of spinal tuberculosis. JBJS Rev 2014;2(09):e4
20 Tuli SM. General principles of osteoarticular tuberculosis. Clin Orthop Relat Res 2002;(398):11–19
21 Jain AK, Dhammi IK, Jain S, Mishra P. Kyphosis in spinal tuberculosis - prevention and correction. Indian J Orthop 2010;44(02): 127–136
22 Rivas-Garcia A, Sarria-Estrada S, Torrents-Odin C, Casas-Gomila L, Franquet E. Imaging findings of Pott's disease. Eur Spine J 2013;22 (suppl 4):567–578
23 Garg RK, Somvanshi DS. Spinal tuberculosis: a review. J Spinal Cord Med 2011;34(05):440–454
24 Shanley DJ. Tuberculosis of the spine: imaging features. AJR Am J Roentgenol 1995;164(03):659–664
25 Hsu LC, Leong JC. Tuberculosis of the lower cervical spine (C2 to C7). A report on 40 cases. J Bone Joint Surg Br 1984;66(01):1–5
26 Abdelwahab IF, Camins MB, Hermann G, Klein MJ. Vertebral arch or posterior spinal tuberculosis. Skeletal Radiol 1997;26(12): 737–740
27 Ansari S, Amanullah MF, Ahmad K, Rauniyar RK. Pott's spine: diagnostic imaging modalities and technology advancements. N Am J Med Sci 2013;5(07):404–411
28 Moorthy S, Prabhu NK. Spectrum of MR imaging findings in spinal tuberculosis. AJR Am J Roentgenol 2002;179(04):979–983
29 Sinha A, Spalkit S, Prabhakar A, Prakash M. Radiology in TB spine (Xrays, ultrasound, CT, MRI). In: Dhatt SS, Kumar V, eds. Tuberculosis of the Spine [Internet]. Singapore: Springer Nature; 2022: 91–112
30 Sharif HS, Morgan JL, al Shahed MS, al Thagafi MY. Role of CT and MR imaging in the management of tuberculous spondylitis. Radiol Clin North Am 1995;33(04):787–804
31 Boxer DI, Pratt C, Hine AL, McNicol M. Radiological features during and following treatment of spinal tuberculosis. Br J Radiol 1992; 65(774):476–479
32 Dhodapkar MM, Patel T, Rubio DR. Imaging in spinal infections: current status and future directions. N Am Spine Soc J 2023; 16:100275
33 Boachie-Adjei O, Squillante RG. Tuberculosis of the spine. Orthop Clin North Am 1996;27(01):95–103
34 Rao BD, Rao KS, Subrhamanian MV, Reddy MV. Granulomatous lesions of the spinal epidural space. Neurol India 1965;13(03): 89–92
35 Srinivasa R, Sai Kiran NA, Hegde AS. Tuberculosis of the spine. Spine J 2016;16(07):e445–e446
36 Gouliamos AD, Kehagias DT, Lahanis S, et al. MR imaging of tuberculous vertebral osteomyelitis: pictorial review. Eur Radiol 2001;11(04):575–579
37 Venkat B, Aggarwal V, Aggarwal N, Sharma S. Imaging features of extraspinal osteoarticular tuberculosis and its mimickers: a review. J Clin Diagn Res 2018;12(07):TE01–TE07

38 Sharma A, Goyal M, Mishra NK, Gupta V, Gaikwad SB. MR imaging of tubercular spinal arachnoiditis. AJR Am J Roentgenol 1997;168 (03):807–812
39 Tu L, Liu X, Gu W, et al. Imaging-assisted diagnosis and characteristics of suspected spinal brucellosis: a retrospective study of 72 cases. Med Sci Monit 2018;24:2647–2654
40 Boudabbous S, Paulin EN, Delattre BMA, Hamard M, Vargas MI. Spinal disorders mimicking infection. Insights Imaging 2021;12 (01):176
41 Kumar Y, Gupta N, Chhabra A, Fukuda T, Soni N, Hayashi D. Magnetic resonance imaging of bacterial and tuberculous spondylodiscitis with associated complications and non-infectious spinal pathology mimicking infections: a pictorial review. BMC Musculoskelet Disord 2017;18(01):244
42 Ahmadi J, Bajaj A, Destian S, Segall HD, Zee CS. Spinal tuberculosis: atypical observations at MR imaging. Radiology 1993;189(02): 489–493
43 Hong SH, Choi JY, Lee JW, Kim NR, Choi JA, Kang HS. MR imaging assessment of the spine: infection or an imitation? Radiographics 2009;29(02):599–612
44 Bron JL, de Vries MK, Snieders MN, van der Horst-Bruinsma IE, van Royen BJ. Discovertebral (Andersson) lesions of the spine in ankylosing spondylitis revisited. Clin Rheumatol 2009;28(08): 883–892
45 Salaffi F, Ceccarelli L, Carotti M, et al. Differentiation between infectious spondylodiscitis versus inflammatory or degenerative spinal changes: how can magnetic resonance imaging help the clinician? Radiol Med (Torino) 2021;126(06):843–859
46 Ledbetter LN, Salzman KL, Sanders RK, Shah LM. Spinal neuroarthropathy: pathophysiology, clinical and imaging features, and differential diagnosis. Radiographics 2016;36(03): 783–799
47 De Backer AI, Vanhoenacker FM, Sanghvi DA. Imaging features of extraaxial musculoskeletal tuberculosis. Indian J Radiol Imaging 2009;19(03):176–186
48 Jangid R, Solanki RS, Chaudhary V, Sud A, Kaur R. Spectrum of imaging findings in osteoarticular tuberculosis. Egypt J Radiol Nucl Med 2024;55(01):23
49 Foocharoen C, Nanagara R, Foocharoen T, Mootsikapun P, Suwannaroj S, Mahakkanukrauh A. Clinical features of tuberculous septic arthritis in Khon Kaen, Thailand: a 10-year retrospective study. Southeast Asian J Trop Med Public Health 2010;41(06): 1438–1446
50 Chattopadhyay A, Sharma A, Gupta K, Jain S. The Phemister triad. Lancet 2018;391(10135):e20
51 Kerri O, Martini M. Tuberculosis of the knee. Int Orthop 1985;9 (03):153–157
52 Salehi M, Manshadi SAD, Yassin Z, Hassannejad M. A simple approach for diagnosis of chronic tuberculous osteomyelitis: a case report. Arch Clin Infect Dis 2017;12(02):e57281
53 Hong SH, Kim SM, Ahn JM, Chung HW, Shin MJ, Kang HS. Tuberculous versus pyogenic arthritis: MR imaging evaluation. Radiology 2001;218(03):848–853
54 Rheumatoid Arthritis and Tuberculous Arthritis. Differentiating MRI Features. Accessed March 29, 2024 at: https://ajronline.org/doi/epdf/10.2214/AJR.08.2164
55 Renson T, Carron P, De Craemer AS, et al. Axial involvement in patients with early peripheral spondyloarthritis: a prospective MRI study of sacroiliac joints and spine. Ann Rheum Dis 2021;80 (01):103–108
56 Bariteau JT, Waryasz GR, McDonnell M, Fischer SA, Hayda RA, Born CT. Fungal osteomyelitis and septic arthritis. J Am Acad Orthop Surg 2014;22(06):390–401
57 Teo HEL, Peh WCG. Skeletal tuberculosis in children. Pediatr Radiol 2004;34(11):853–860
58 Murphy MC, Murphy AN, Hughes H, McEneaney OJ, O'Keane C, Kavanagh E. Multimodal imaging of Spina Ventosa (TB Dactylitis) of the foot. Radiol Case Rep 2020;15(08):1373–1376
59 Hamard A, Burns R, Miquel A, et al. Dactylitis: a pictorial review of key symptoms. Diagn Interv Imaging 2020;101(04):193–207
60 Jaovisidha S, Chen C, Ryu KN, et al. Tuberculous tenosynovitis and bursitis: imaging findings in 21 cases. Radiology 1996;201(02): 507–513
61 Tuberculous Infection of the Wrist. MRI Features. Accessed March 30, 2024 at: https://www.ajronline.org/doi/epdf/10.2214/ajr.183.3.1830623
62 Kim JH, Lee JS, Choi BY, et al. Isolated tuberculous myositis: a systematic review and multicenter cases. J Rheum Dis 2022;29 (04):243–253
63 Sharma SK, Ryan H, Khaparde S, et al. Index-TB guidelines: guidelines on extrapulmonary tuberculosis for India. Indian J Med Res 2017;145(04):448–463
64 Mittal S, Jain AK, Chakraborti KL, Aggarwal AN, Upreti L, Bhayana H. Evaluation of healed status in tuberculosis of spine by fluorodeoxyglucose-positron emission tomography/computed tomography and contrast magnetic resonance imaging. Indian J Orthop 2019;53(01):160–168
65 Mann TN, Davis JH, Beltran C, et al. Evaluation of host biomarkers for monitoring treatment response in spinal tuberculosis: a 12-month cohort study. Cytokine 2022;157:155944

